AFRL-SA-WP-TR-2016-0011

Prolonged Hypobaria during Aeromedical Evacuation and the Effects on Traumatic Brain Injury

Gary Fiskum, PhD

January 2016

Final Report
for October 2011 to October 2014

Air Force Research Laboratory
711th Human Performance Wing
U.S. Air Force School of Aerospace Medicine
Aeromedical Research Department
2510 Fifth St., Bldg. 840
Wright-Patterson AFB, OH 45433-7913

NOTICE AND SIGNATURE PAGE

Using Government drawings, specifications, or other data included in this document for any purpose other than Government procurement does not in any way obligate the U.S. Government. The fact that the Government formulated or supplied the drawings, specifications, or other data does not license the holder or any other person or corporation or convey any rights or permission to manufacture, use, or sell any patented invention that may relate to them.

Qualified requestors may obtain copies of this report from the Defense Technical Information Center (DTIC) (http://www.dtic.mil).

AFRL-SA-WP-TR-2016-0011 HAS BEEN REVIEWED AND IS APPROVED FOR PUBLICATION IN ACCORDANCE WITH ASSIGNED DISTRIBUTION STATEMENT.

//SIGNATURE//	//SIGNATURE//
COL NICOLE ARMITAGE	DR. RICHARD A. HERSACK
Chief, En Route Care Research Division	Chair, Aeromedical Research Department

This report is published in the interest of scientific and technical information exchange, and its publication does not constitute the Government's approval or disapproval of its ideas or findings.

REPORT DOCUMENTATION PAGE

Form Approved
OMB No. 0704-0188

1. REPORT DATE *(DD-MM-YYYY)*	2. REPORT TYPE	3. DATES COVERED *(From – To)*
28 Jan 2016	Final Technical Report	October 2011 – October 2014

4. TITLE AND SUBTITLE

Prolonged Hypobaria during Aeromedical Evacuation and the Effects on Traumatic Brain Injury

5a. CONTRACT NUMBER
FA8650-11-2-6D04

5b. GRANT NUMBER

5c. PROGRAM ELEMENT NUMBER

6. AUTHOR(S)
Gary Fiskum, PhD

5d. PROJECT NUMBER

5e. TASK NUMBER

5f. WORK UNIT NUMBER

7. PERFORMING ORGANIZATION NAME(S) AND ADDRESS(ES)
USAF School of Aerospace Medicine
Aeromedical Research Department/FHE
2510 Fifth St., Bldg. 840
Wright-Patterson AFB, OH 45433-7913

8. PERFORMING ORGANIZATION REPORT NUMBER

AFRL-SA-WP-TR-2016-0011

9. SPONSORING / MONITORING AGENCY NAME(S) AND ADDRESS(ES)

10. SPONSORING/MONITOR'S ACRONYM(S)

11. SPONSOR/MONITOR'S REPORT NUMBER(S)

12. DISTRIBUTION / AVAILABILITY STATEMENT

DISTRIBUTION STATEMENT A. Approved for public release.

13. SUPPLEMENTARY NOTES
Cleared, SAF/PA, Case # 2016-0437, 28 Sep 2016.

14. ABSTRACT

In response to concerns by Critical Care Air Transport Teams that prolonged flights during aeromedical evacuation (AE) of neurotrauma patients might worsen neurologic outcomes, the effects of exposing rats to hypobaria (HB) at different times after mild or moderate traumatic brain injury (TBI) were investigated. Following either impact-induced moderate TBI or blast-induced mild TBI, histologic and neurologic markers of injury were worsened by 6 hours HB (=8,000 feet altitude), initiated at 6, 24, or 72 hours after injury or 6-7 days after injury. Brain injury was also worse when rats were exposed to 100% oxygen (O_2) compared to 21-28% O_2 during HB. Exposure to two flights at 24 hours and 72 hours caused more damage than one flight at either of these times following impact TBI but not blast TBI. Following impact TBI, administration of CR8, an anti-inflammatory cell cyclin-dependent kinase inhibitor, improved behavioral and histologic outcomes. TBI and subsequent HB were accompanied by elevated levels of serum microparticles, which could contribute to systemic inflammation. Changes in gene expression in the brain following blast TBI and HB suggest that drugs that trigger an increase in the expression of cytoprotective genes could be used to improve outcomes in these paradigms. These results support the hypothesis that exposure to AE-relevant HB within a few days after TBI can be dangerous. They also suggest that levels of inspired O_2 during AE should not be greater than those necessary to maintain systemic normoxia.

15. SUBJECT TERMS
Hypobaria, traumatic brain injury, TBI, aeromedical evacuation, normoxia, hyperoxia, inflammation

16. SECURITY CLASSIFICATION OF:			17. LIMITATION OF ABSTRACT	18. NUMBER OF PAGES	19a. NAME OF RESPONSIBLE PERSON
a. REPORT	b. ABSTRACT	c. THIS PAGE			Gary Fiskum, PhD
U	U	U	SAR	43	19b. TELEPHONE NUMBER *(include area code)*

Standard Form 298 (Rev. 8-98)
Prescribed by ANSI Std. Z39.18

This page intentionally left blank.

TABLE OF CONTENTS

Section **Page**

LIST OF FIGURES

Page

LIST OF TABLES

Page

ACKNOWLEDGMENTS

The following individuals contributed significantly to this project:

- Faculty – Gary Fiskum, Alan Faden, Joseph Dubose, Raymond Fang, William Fourney, Ulrich Leist, Robert Rosenthal, Adam Puche, Shruti Kabadi, Junfang Wu

- Postdoctoral fellows and students – Jacob Skovira (PhD dissertation), Yi-Chun Hsieh (postdoc)

- Research staff – Zaorui Zhao, Julie Proctor, Joshua Vaughan, Dominique Scutella

This page intentionally left blank.

1.0 SUMMARY

In response to concerns by Critical Care Air Transport Teams that prolonged flights during aeromedical evacuation (AE) of neurotrauma patients might worsen neurologic outcomes, the effects of exposing rats to hypobaria (HB) at different times after mild or moderate traumatic brain injury (TBI) were investigated. Following either impact-induced moderate TBI or blast-induced mild TBI, histologic and neurologic markers of injury were worsened by 6 hours HB (=8,000 feet altitude), initiated at 6, 24, or 72 hours or 6-7 days after injury. Brain injury was also worse when rats were exposed to 100% oxygen compared to 21-28% oxygen during HB. Exposure to two flights, at 24 hours and 72 hours, caused more damage than one flight at either of these times following impact TBI but not blast TBI. Following impact TBI, administration of CR8, an anti-inflammatory cyclin dependent kinase inhibitor, improved behavioral and histologic outcomes. TBI and subsequent HB were accompanied by elevated levels of serum microparticles, which could contribute to systemic inflammation. Changes in gene expression in the brain following blast TBI and HB suggest that drugs that trigger an increase in the expression of cytoprotective genes could be used to improve outcomes in these paradigms. These results support the hypothesis that exposure to AE-relevant HB within a few days after TBI can be dangerous. They also suggest that levels of inspired oxygen during AE should not be greater than those necessary to maintain systemic normoxia. The results obtained with CR8 treatment provide proof-of-principle that pharmacologic approaches can be used to mitigate the adverse effects of AE-relevant HB on TBI.

2.0 INTRODUCTION

The principal purpose of this agreement was to perform pre-clinical research directed at optimizing the transport and care of critically injured patients. This effort was focused on innovative technology concepts to capitalize on advances in aerospace medicine and to enhance aeromedical care and expeditionary medicine capabilities. These enhancements will improve traumatically injured patient support in the public sector, and the resulting research will transition to appropriate military applications while improving the survival rate of combat forces. Work was conducted at the University of Maryland School of Medicine and at the University of Maryland R Adams Cowley Shock Trauma Center. Investigators included Dr. Joseph DuBose and Dr. Raymond Fang from the Center for the Sustainment of Trauma and Readiness Skills (C-STARS) Baltimore, Drs. Gary Fiskum, Alan Faden, Robert Rosenthal, and Adam Puche from the University of Maryland School of Medicine Center for Shock, Trauma, and Anesthesiology Research, and Dr. William Fourney from the University of Maryland School of Engineering

Traumatic brain injury (TBI) is a very common cause of injury and death in patients presenting to emergency care in military settings. Many of these patients are aeromedically evacuated from theatre to Landstuhl Regional Medical Center and subsequently to the United States. Although it is assumed that rapid evacuation to higher levels of care is beneficial to the TBI victim, aeromedical evacuation (AE) is not without independent risk factors, including exposure to hypobaria (HB), which can increase intracranial pressure and reduce cerebral blood flow.

Our proposal applies rigorously controlled basic science research to verify if and how exposure to prolonged HB at different times after TBI worsens long-term histologic, neurochemical, and behavioral outcomes. The knowledge gained will be critical for the further

development of evidence-based clinical practice air evacuation protocols for long-distance, high-altitude evacuation, including the development and deployment of novel, appropriate, and robust neuroprotection strategies, and so has important potential benefit for both civilian and military populations.

3.0 BACKGROUND

Just as TBI became the signature injury of Operation Iraqi Freedom and Operation Enduring Freedom, the ability to provide rapid advanced care for trauma patients has been recognized as the key component contributing to survival of critically injured casualties. Casualties are now evacuated rapidly to central hospitals capable of providing advanced levels of resuscitative and surgical care. Once stabilized (24-48 hours), patients are transported with critical care teams aboard specially equipped C-17 transport planes to Landstuhl Regional Medical Center. When all injuries are identified and initial treatment started, the patient is evacuated to the United States, often within a few days of injury.

Although it is assumed that rapid evacuation to higher levels of care will be beneficial to the TBI victim, the actual transport is not without independent risk factors. Multiple environmental variables during transport, including temperature, noise, vibration, interruption of sleep cycles, etc., may affect the delicate physiological homeostasis required for recovery from TBI. Of particular interest is the effect of changes in ambient pressure during air transport. Even "pressurized" aircraft are maintained at 576 mmHg (8,000 feet above sea level). The effects of such HB have been well studied but not in TBI patients, where hypobaric conditions could theoretically worsen cerebral ischemia and hypoxia. One very important study performed with a weight-drop, mouse TBI model demonstrated that exposure to 5 hours of HB at 3 but not 24 hours after injury increased a serum marker of neuronal injury (neuron-specific enolase) and both serum and brain inflammatory cytokines within 24 hours after injury [1]. Long-term neurologic and histologic outcomes were not reported, however.

We hypothesized that the combination of lower inspired oxygen (O_2) and mild edema associated with AE-relevant HB exacerbates TBI due to worsening of axonal injury, neuronal death, inflammation, and oxidative stress. We also hypothesized that the effects of HB are either qualitatively or quantitatively different following TBI of mild vs. moderate severity. We further hypothesized that exposure of animals to severe hyperoxia (100% O_2) during HB following TBI would worsen rather than improve outcomes, compared to exposure to 21-28% O_2. Finally, we tested the ability of a novel anti-inflammatory agent to improve outcomes following moderate TBI and subsequent HB.

4.0 METHODS

4.1 Exposure to AE-Relevant HB

Hypobaria was induced using a steel cylindrical chamber with interior dimensions of 46 cm wide and 112 cm long equipped with internal temperature, oxygen, carbon dioxide, and pressure gauges and connected to a vacuum pump. In general, four adult male Sprague-Dawley rats (250 – 350 g) were placed into the chamber in two cages, with access to water and food. The chamber was depressurized over 30 minutes to reach 568 mmHg (=8,000 feet altitude) approximating the cabin pressure during military AE with cruising altitudes of 30,000 –

40,000 feet. The gas entering the chamber was maintained throughout the flight at either 21%, 28%, or 100% O_2. Chamber gases were continuously monitored to validate concentration of O_2 delivered, as well as to verify that expired carbon dioxide was not accumulating in the chamber. At 5.5 hours of HB, the chamber was repressurized over 30 minutes to 1 atm (765 mmHg). The animals were then removed and returned to their home cages. Interior chamber temperature was monitored continuously and maintained at 22 ± 2°C.

4.2 Underbody Blast-Induced Mild TBI Caused by Hyperacceleration

All experiments and analyses using this model were performed in the laboratory of Dr. Gary Fiskum.

The device used to induce underbody blast-induced acceleration consisted of an aluminum water tank 3 feet long x 2 feet wide x 2 feet deep in which a platform was located that supported two aluminum plates, each 15 in^2 and 1.5 inches thick. The two plates were separated by a styrofoam or rubber pad of the same dimensions that absorbed some of the force transmitted between the plates. The plates and pad travel vertically in response to a blast in the water tank, guided by poles located in holes in each corner of the plates and pad. Two cylinders were secured to the top of the plate. Each cylinder contained one prone, ketamine-anesthetized rat, covered by six layers of 100% cotton batting. Batting used in experiments contained a scrim binder and each layer was approximately 1/8 inch thick. An additional four layers of batting were placed under the chin of the rat to minimize secondary head movement within the cylinder. Under these conditions, the movements of the rat within the cylinder following the blast were severely restricted, as evidenced by ultra-high-speed cinematography.

An explosive charge of 0.75 g pentaerythritol tetranitrate was placed in the water precisely under the center of the plate at a distance that generated a mean maximal G-force of 100 ± 15 standard error of the mean, as measured by an accelerometer bolted to the top plate immediately next to the head-end of the cylinder. When detonated, the explosion caused the plate containing the two rats to accelerate upward extremely rapidly to a height of < 4 inches, followed by return to the original location. More information can be found in the publication by Proctor et al. [2].

4.2.1 Silver Staining of Damaged Axons and Immunohistochemical Staining of Immunoglobulin G Blood Brain Barrier Disruption. At 30 days post-blast, rats were heavily anesthetized by intraperitoneal (IP) injection of ketamine (160 mg/kg) and xylazine (20 mg/kg). Rats were transcardially perfused with artificial cerebrospinal fluid solution (148 mM sodium chloride, 3 mM potassium chloride, 1.85 mM calcium chloride, 1.7 mM magnesium chloride, 1.5 mM disodium phosphate, 0.14 mM monosodium phosphate, 5 mM glucose, pH 7.4) oxygenated with 100% O_2 (beginning 30 minutes prior to perfusion and continuing during the perfusion) at the rate of 25-30 mL/min for 5 minutes. This physiologic flush was followed immediately by perfusion with a 4% paraformaldehyde solution at the rate of 25-30 mL/min for 20 minutes. Brains were removed from the skull, and those designated for electron microscopy were subjected to secondary fixation in a mixture of 4% paraformaldehyde and 1% glutaraldehyde with 0.1 M phosphate buffer pH 7.4 for 48 hours at 4°C. All other brains were removed and transferred into 30% sucrose. Once brains sunk to the bottom of the container, they were cut (40 μm) on a freezing sliding microtome, yielding 24 series per animal, and kept in cryoprotectant (-20°C) until further processing was initiated.

The amino cupric silver method of de Olmos was used to stain free-floating 40-µm tissue for the identification of damaged and degenerating axons. Our staining procedure closely followed the detailed protocol described by Tenkova and Goldberg [3]. Prior to staining, all glassware was cleaned in 50% nitric acid. Sections were rinsed free from cryoprotectant and incubated in 4% paraformaldehyde (4°C) for 1 week prior to staining to block non-specific labeling of neurons. Sections were then rinsed with deionized water and incubated in pre-impregnation buffer (cupric-silver) for 1 hour at 50°C then at room temperature overnight. The next day, sections were exposed to the following solutions at room temperature: 100% acetone (30 seconds), impregnation buffer (silver-diamine) solution for 35 minutes, reduction agent (formaldehyde with citric acid) for 2 minutes, bleaching solution (potassium ferricyanide) for 20 minutes, deionized water for 3 minutes, and stabilization buffer (thiosulfate solution) for 10 minutes. All solutions were made fresh immediately before use, and sections were carefully shielded from direct light during all staining procedures. After staining, sections were mounted in 50% ethanol onto subbed PLUS slides, dehydrated with ethanol and xylene, and subsequently coverslipped with DPX mounting media.

To quantify silver-stained injured axons, we utilized unbiased optical dissector methodologies. Sections containing the internal capsule (corresponding to bregma -1.80 mm) were examined using bright field illumination at 100x magnification. A 25- x 25-µm grid was superimposed over the tissue using Neurolucida reconstruction software (MBF Bioscience, Williston, VT), and five squares within that grid were randomly chosen for counting by a microscopist who was blinded to the identity of the tissue mounted on the slides. The number of axons crossing one side from each of the five squares into the volume of the counting square was then counted. Typical top-upper-right exclusion and bottom-lower-left inclusion boundaries for unbiased optical dissector stereology approaches were utilized.

Many forms of TBI result in brain parenchymal immunoglobulin G (IgG) immunostaining, based on disruption of tight junctions between vascular endothelial cells, resulting in leakage of IgG from the blood into the parenchyma. Forty-µm free-floating, fixed brain sections were rinsed in Tris-buffered saline (TBS) for 30 minutes, incubated with 1% sodium borohydrate for 20 minutes, treated with TBS containing 10% methanol and 1% hydrogen peroxide for 10 minutes, blocked with bovine serum albumin in TBS containing 0.3% Triton X-100 (TBST) for 1 hour, and subsequently incubated with biotinylated goat anti-rat IgG (H+L) (1:5K; Vector Laboratories, Burlingame, CA) overnight at 4°C. The sections were then incubated with ABC kit (1:222, Vector Laboratories) for 1 hour at room temperature and developed with nickel sulfate enhanced 3,3'-diaminobenzidine (Ni-DAB). Sections were then mounted on gelatin-coated glass slides, dehydrated in ethanol series, cleared in histoclear, and subsequently coverslipped with histomount.

The histological examination and analysis of IgG effusions were performed with microscope slides containing brain sections that were blinded to the microscopist. The damaged microvessels were recognized as IgG immunoreactivity forming oval or circular shape around the vessels. Sampling was performed in 0.169 mm^2 boxes placed in the sensory and motor cortex regions and image acquired using a Nikon Eclipse E800 microscope (Melville, NY) under 20x magnification plus image acquisition software Stereo Investigator 10 (MBF Bioscience, Williston, VT). The images were further analyzed using ImageJ. A sampling line crossing the center of the IgG immunoreactive circle was drawn perpendicular to the blood vessel to obtain the densitometry of the IgG immunostaining and the diameter of the IgG effusion area thus measured. The level of brain blood barrier compromise was further calculated as percent

investigated area covered by IgG effusion determined by the measured size of the effusion and the number of IgG events occurred per mm^2.

4.2.2 Vestibulomotor Performance: Beam Tasks. The beam balance test is a common and well-established method used to evaluate motor function following TBI in rodents. Briefly, the beam test consisted of placing the rat on an elevated (100 cm) narrow (2.0 cm wide) wooden beam and recording the number of foot slips and the time it takes the rat to traverse the beam.

Two days prior to blast experiments, rats were trained to traverse the beam using a negative-reinforcement paradigm where rats are able to escape light and white noise by traversing an elevated narrow beam (2.0 × 120 cm) into a darkened goal box situated at the opposite end of the beam. A 2-inch-thick slab of foam was placed directly beneath the beam as padding in case the rat fell from the beam. Rats were initially placed inside the darkened goal box for 60 seconds, after which a white noise generator (ANY-maze software, Stoelting Co., Wood Dale, IL) was turned on and the rat taken out of the box and placed on the beam approximately 50 cm (halfway point on beam) from the goal box. Once the rat crossed the beam and entered the darkened box, the noise ceased and the rat remained in the box for 30 seconds. This process was repeated at approximately 75 cm and 100 cm from the box with 30-second quiet timeouts in the box in-between training sessions. Rats were then placed at the starting point (100 cm from the box) and latency to cross the beam was recorded. Rats were considered "trained" once they could traverse the entire length of the beam in under 5 seconds, 3 times in a row. Crossings were repeated as many times as necessary until this goal was reached (usually 8-10 crossings were sufficient to reach this goal). Rats that did not perform tasks without errors (traverse the beam in under 5 seconds, 3 times in a row) were excluded from experiments.

The first testing phase (baseline) occurred 24 hours after the training phase and 24 hours prior to blast experiments. Rats were then assessed on day 7 post-injury for beam balance performance. Testing consisted of three beam crossings where latency to cross and number of foot slips during crossing were recorded. As in the training phase, once rats entered the darkened goal box, the white noise generator was turned off and rats remained in the box for 30 seconds in-between trials.

4.3 Lateral Fluid Percussion Model of Moderate TBI

All experiments and analyses using this animal model were performed in the laboratory of Dr. Alan Faden.

Rats were anesthetized with isoflurane (4% induction, 2% maintenance) evaporated in a gas mixture containing 70% room air and 30% O_2 administered through a nose cone. The surgical site on the scalp was cleared of hair with small animal electric clippers and the animal's head was mounted in a stereotaxic frame. A surgical plane of anesthesia was confirmed by a lack of eye reflexes and withdrawal response to a foot pinch. A sterile petrolatum ophthalmic lubricant (Puralube vet ointment) was applied to form a protective film over the ocular surface, lubricate the eye, and protect the eye from drying. The surgical site was then cleaned three times alternating with a povidone-iodine prep pad and 70% isopropyl alcohol pads and covered with a sterile drape. A midline incision was made to expose the craniotomy site and the skin and fascia were reflected. A 5-mm craniotomy was made over the left parietal cortex midway between lambda and bregma using a small drill with a sterile bit. A luer lock female adaptor was secured to the craniotomy site using superglue and dental acrylic to facilitate connection with the micro-

fluid percussion (FP) device for the injury induction. Following injury, the incision was closed with surgical staples. Anesthesia was then terminated and the animal was placed into a heated recovery chamber and monitored for 1 hour post-surgery before being returned to its home cage. The animal's systemic temperature was maintained at 37.0 ± 0.5°C through use of a circulating water heating pad. Sham animals underwent the same procedure as injured rats with the exception of the micro-FP impact.

The female luer lock attached to the craniotomy site on the skull was fit into a male luer lock adaptor of a custom micro-FP device, which is a microprocessor-controlled, pneumatically driven device consisting of a microprocessor-controlled initiator assembly, an air-driven impactor, and pressure chamber. When the device is triggered, the pneumatic cylinder extends and impacts the piston, causing the transfer of impact energy to the fluid in the pressure chamber resulting in a pressure wave released from the chamber directly onto the exposed dura. The pressure is recorded by a pressure transducer on the bottom of the fluid chamber and displayed on a laptop using the Powerlab data acquisition system through the Chart4 Windows 4.2 software program. The degree of injury is directly related to the pressure wave expressed in atmospheres. A 1.5- to 1.9-atm pressure was used to produce a mild injury with regard to neurologic and histologic deficits.

4.3.1 Histology. At 30 days post-HB, rats were anesthetized with sodium pentobarbital (100 mg/kg IP) and transcardially perfused with saline followed by 4% paraformaldehyde. The brains were removed, placed in 4% paraformaldehyde for 24 hours, and then cryoprotected in 30% sucrose. Brains were serially sectioned (60 μm and 20 μm) on a cryostat and mounted onto glass slides. Selected slides were stained with cresyl violet (FD Neurotechnologies, Columbia, MD) for hippocampal neuronal cell counts and lesion volume analysis or with a polyclonal anti-ionized calcium-binding adapter molecule 1 (Iba-1) antibody (Wako Chemicals, Richmond, VA) for cortical microglial cell counts.

4.3.1.1 Assessment of Microglial Morphology in the Ipsilateral Cortex. Brain sections obtained as described above were immunostained for the microglia marker Iba-1. The number of cortical microglia in either activated or resting morphologic phenotypes was counted using the optical fractionator method of unbiased stereology with Stereo Investigator software (MBF Bioscience) as described by Byrnes et al. [4] and Kabadi et al. [5] (n=5-12/group). The sampling region was between -2.04 mm and -4.56 mm from bregma in the ipsilateral cortex with a dorsal depth of 2.0 mm from the surface. Every fourth 60-μm section was analyzed. Sections were analyzed using a Leica DM4000B microscope (Leica Microsystems Inc., Buffalo Grove, IL). The optical dissector had a size of 50 μm in the x and y axes with a height of 10 μm and guard zone of 4 μm from the top of the section. Dissectors were positioned every 150 μm in the x and y axes. Microglial phenotypic classification was based on the length and thickness of the projections, the number of branches, and the size of the cell body as described previously [4,5]. The volume of the region of interest was measured using the Cavalieri estimator method. The estimated number of microglia in each phenotypic class was divided by the volume of the region of interest to obtain cellular density expressed in counts/mm^3.

4.3.1.2 Hippocampal Neuronal Cell Loss. Brain sections obtained as described above were stained with cresyl violet (FD Neuro Technologies), dehydrated, and mounted for analysis (n=4-10/group). Neuronal cell loss was quantified with Stereo Investigator software (MBF Biosciences) as described by Byrnes [4] to count the total number of surviving neurons in the Cornu Ammonis (CA)1, CA2, CA3, and dentate gyrus subregions of the hippocampus using the optical fractionator method of unbiased stereology. Every fourth 60-μm section between -2.04 mm and -4.56 mm from bregma was analyzed, beginning from a random start point. The optical dissector had a size of 50 μm by 50 μm in the x- and y-axis, respectively, with a height of 10 μm and a guard-zone of 4 μm from the top of the section. The sampled region for each hippocampal subfield was demarcated in the injured hemisphere, and cresyl violet neuronal cell bodies were counted. For each subregion, a grid spacing of 400 μm in the x-axis and 400 μm in the y-axis was used, resulting in an area fraction of 164^{th}. The volume of each hippocampal subfield was measured using the Cavalieri estimator method with a grid spacing of 50 μm. The estimated number of surviving neurons in each field was divided by the volume of the region of interest to obtain the neuronal cellular density, expressed as counts/mm^3.

4.3.1.3 Lesion Volume in the Ipsilateral Cortex. Brain sections obtained as described above were stained with cresyl violet (FD Neuro Technologies), dehydrated, and mounted for analysis (n=4/group). Lesion volume was quantified based on the Cavalieri method of unbiased stereology using Stereo Investigator software (MBF Biosciences). The lesion volume was quantified by outlining the missing tissue on the injured hemisphere using the Cavalieri estimator with a grid spacing of 0.1 mm. From 96 total 60-μm sections, every eighth section was analyzed beginning from a random start point.

4.3.2 Neurobehavioral Tests

4.3.2.1 Composite Neuroscore. Standardized motor scoring was performed at 1, 7, 14, and 21 days after HB exposure. Motor function was evaluated using three separate tests, each of which was scored via an ordinal scale ranging from 0 (severely impaired) to 5 (normal function). The tests include the ability to maintain position on an inclined plane in the vertical and two horizontal positions for 5 seconds (forelimb flexion and forced lateral pulsion). The first test measured the reflex extension of the forelimb to break a fall when suspended by the tail. Forelimb contraflexion was assessed by temporarily suspending the rat by the tail above a flat surface and assigning a score based on the position of the head, shoulders, and paws in response to this perceived fall. The second test measured the animals' ability to resist a lateral push. Finally, animals were tested on their ability to stand on an angle board (30-70 angle) positioned head up and right and left horizontal positions. Each test was rated 0 to 5. Each of seven individual scores (vertical angle, right and left horizontal angle, right and left forelimb flexion, right and left lateral pulsion) was added to yield a composite neurological score ranging from 0 to 35.

4.3.2.2 Morris Water Maze. Spatial learning and memory were assessed by using the acquisition paradigm of the Morris water maze (MWM) test on post-HB days 14, 15, 16, and 17. A circular pool (1.5 meters in diameter) was divided into four quadrants, northwest, northeast, southwest, and southeast, using computer-based ANY-maze video tracking system (Stoelting Co.), and non-toxic white paint was used to color the water so a platform could be hidden in one

of the quadrants (southwest) 14 inches from the side wall. Each rat was subjected to four trials to locate the hidden platform every day from post-HB days 14-17 (acquisition phase); the rat was introduced into the apparatus from a different quadrant for every trial, and order of introduction varied across the trial days. The cognitive outcomes were determined in terms of latency (seconds) to locate the hidden platform with a 90-second limit per trial. In addition, distance traveled and swimming velocities were assessed. Water maze search strategy analysis was also performed. Three strategies were identified using a categorization scheme: 1) spatial strategies were defined as swimming directly to platform with no more than 1 loop or swimming directly to the correct target quadrant and searching, 2) systematic strategies were defined as searching the interior portion or the entire tank without spatial bias and searching incorrect target quadrant, and 3) looping strategies were defined as circular swimming around the tank, swimming in a tight circle, and swimming around the wall of the tank. The search strategies were analyzed on all acquisition trials on post-HB day 17, and a percentage of each strategy in each group was calculated. Reference memory was assessed by a probe trial carried out on post-HB day 18. For this trial, the platform was removed from the apparatus. The rat was then introduced into the apparatus from the northeast quadrant and the animal was allowed to search with a 60-second limit. A visual cue test was performed on post-HB day 18 by using a flagged platform placed in one of the quadrants to ensure visual acuity of all animals with a 90-second limit per trial, and latency (seconds) to locate the flagged platform was recorded.

4.3.2.3 Novel Object Recognition. Non-spatial retention and recognition memory were assessed by the novel object recognition test on post-HB day 21. The apparatus consisted of an open field (60 cm x 24 cm x 45.4 cm). Using the computer-based ANY-maze video tracking system (Stoelting Co.), two circular zones were created equally spaced from the sides and in the center of the apparatus. The zones were designated as the “old object” and “novel object” zones. The objects used were assembled from LEGO-DUPLO building blocks and were clearly distinct in their shape and appearance. The “old object” used was square shaped, whereas the “novel object” was triangular. On post-HB day 20, animals were placed into the open field and allowed to explore for 10 minutes each without any of the objects present for habituation and familiarization. On the testing day (post-HB day 21), two trials of 5 minutes each were performed. The first trial (training phase) involved placing identical square-shaped “old objects” in both zones of the open field. There was then an inter-trial interval of 60 minutes, during which the animals were placed back into their cages. The second trial (testing phase) involved placing one square-shaped “old object” and one triangular-shaped “novel object” in respective zones of the open field. The time that was spent exploring each object during both trials was recorded. In addition, time spent in “novel object” and “old object” zones was analyzed and compared between groups separately.

The cognitive outcomes were calculated as the “discrimination index” (D.I.) for the second trial using the following formula:

% D.I. = [(Time spent exploring novel object/(Total time spent exploring both objects)] x 100

4.3.2.4 Forced Swim Test. The forced swim test was used to examine depressive-like behaviors. On post-HB day 26, rats were individually forced to swim inside a vertical plastic container (height: 60 cm; diameter: 25 cm) containing 30 cm of water for a time period of 6 minutes. The total duration of immobility (passive floating, slightly hunched, upright position,

the head just above the surface) vs. struggle (diving, jumping, strongly moving all four limbs, scratching the walls) was recorded.

4.3.3 Serum Biomarkers

4.3.3.1 Serum Collection. At 24 hours post-injury, rats were injected with 100 mg/kg IP of euthasol using a 25-gauge needle. Adequate anesthesia was determined by the eye blink and tail pinch methods. An incision was then made through the sternum with a pair of surgical scissors and the rib cage was lifted to expose the heart. The heart was then released from the surrounding tissue. A 23g x 1-inch needle was inserted into the left ventricle and 1 mL of blood was collected. The needle was removed from the syringe prior to transfer of the blood into a 13- x 100-mm lithium heparin (90 USP) hemogard closure tube (Fisher Scientific, Pittsburgh, PA) and placed on ice. Serum was extracted from the blood samples by centrifugation at 1000 x G and 4°C for 10 minutes. The serum was then carefully removed with a pipette so as not to include any red or white blood cells and stored at -80°C until analysis.

4.3.3.2 Microparticle Acquisition and Quantification. Serum collected as previously described was suspended in 0.2 M ethylenediaminetetraacetic acid to diminish *ex vivo* microparticle (MP) aggregation. Flow cytometry was performed with a10-color FACSCanto (Becton Dickinson, San Jose, CA) using standard acquisition software. Events were counted based on light scatter, with gates set to include 0.3- to 6.5-µm particles, excluding background corresponding to debris usually present in buffers. MPs were stained with annexin V antibody and analyzed. Samples also included 0.3-µm-diameter (Sigma) and 1.0-, 3.0-, and 6.5-µm-diameter (Spherotech, Lake Forest, IL) microbeads, which were used for initial settings and before each experiment to estimate MP diameters. Analysis involved establishing true-negative controls by a fluorescence-minus-one analysis and by using isotype-matched irrelevant antibodies at the same concentration and under the same conditions. Forward and side scatter was set at logarithmic gain. The absolute numbers of MPs per milliliter of plasma were determined by counting the proportion of beads and the exact volume of plasma from which MPs were analyzed (n=6-10/group).

4.3.4 Brain Tissue Biomarkers

4.3.4.1 Cytokines. Cytokine levels were assayed following the manufacturer's instructions (n=6-10/group) using a multiplex enzyme-linked immunosorbent assay (ELISA) (Q-Plex™, Quansys Biosciences, Logan, UT) allowing the concurrent measurement of nine analytes (interleukin (IL)-1α, IL-1β, IL-2, IL-4, IL-6, IL-10, IL-12p70, interferon gamma (IFN-γ), tumor necrosis factor α). Protein was extracted from ipsilateral cortex tissue in ice-cold 1X phosphate buffered saline containing a protease inhibitor cocktail (10 µl/mL, Sigma-Aldrich, St. Louis, MO) and DNase (50 µg/mL, Sigma-Aldrich) using dounce homogenization. Insoluble debris was separated by centrifugation at 10,000 x g for 20 minutes at 4°C. The supernatant was transferred to sterile microcentrifuge tubes on ice and the protein concentration was determined using the Pierce BCA Protein Assay Kit (Thermo Scientific, Rockford, IL). Aliquots with a protein concentration of 1 mg/mL were then prepared from the samples to assay cytokine levels. Antigen standards were reconstituted using Q-Plex Array sample diluent and the standard curve was prepared according to the antigen standard card provided in the kit. The prepared sample aliquots were diluted 1:2 (parts:total) with sample diluent in a 96-well plate. The Q-Plex Array

96-well plate was washed six times with 1X wash buffer, and 50 µL per well of the standards/diluted samples were loaded into the plate. A seal was applied and the plate was shaken for 3 hours at 500 rpm. The plate was then washed three times with 1X wash buffer; 50 µL per well of detection mix was added, sealed, and shaken for 90 minutes at 500 rpm. After 90 minutes, the plate was washed three times with 1X wash buffer; 1X Streptavidin-horseradish peroxidase (HRP) was added (50 µL per well), sealed, and shaken for 15 minutes at 500 rpm. The plate was then washed six times with 1X wash buffer, then 50 µL per well of mixed substrate was added and imaged immediately using the Bio-Rad ChemiDoc™ XRS+ system (Hercules, CA). Cytokines were quantified by densitometric analysis using the provided Q-View software.

4.3.4.2 Oxyblot Immunoblot. All procedures for the derivatization of protein carbonyls with dinitrophenylhydrazine (DNPH) and subsequent detection using the Oxyblot kit follow the procedure outlined in the kit brochure (n=6-8/group). All immunoblot sample cortical tissue was homogenized in radioimmunoprecipitation assay (RIPA) buffer containing protease and phosphatase inhibitors (10 µl/mL, Sigma-Aldrich) and centrifuged at 15,000 rpm for 15 minutes at 4°C to isolate proteins, and protein concentration was determined using the Pierce BCA Protein Assay Kit (Thermo Scientific). Twelve percent sodium dodecyl sulfate (SDS) (6% v/v final) was added to 12.5 µg protein to denature the protein. Then 1 x DNPH was added to each sample at a 1:1 (v/v) ratio and incubated at room temperature for 15 minutes to derivatize the protein. Neutralization solution was then added to all samples to stop the reaction, followed by the addition of 2-mercaptoethanol (5% v/v final) to reduce the protein. The samples were then loaded and run on 4-12% polyacrylamide gels and the proteins transferred to nitrocellulose membranes. The membranes were blocked with blocking buffer for 1 hour, incubated with the primary antibody at a 1:150 dilution in blocking buffer for 1 hour, washed with phosphate buffered saline Tween 20, and incubated with the secondary antibody at a 1:300 dilution in blocking buffer for 1 hour. After washing, chemiluminescent substrate was added (SuperSignal West Dura Extended Duration Substrate, Thermo Scientific, Rockford, IL) to the membranes and the membranes were imaged using the Kodak Image Station 4000R (Carestream Health, Rochester, NY). Protein bands were quantified by densitometric analysis using the Carestream molecular imaging software. Membranes were then stripped, washed, blocked, and probed with glyceraldehyde-3-phosphate dehydrogenase (GAPDH) (1:2000, Sigma-Aldrich), followed by incubation with Anti-Mouse IgG (1:2000, KPL, Inc., Gaithersburg, MD) for 1 hour. The membranes were then washed and developed as previously indicated.

4.3.4.3 Western Immunoblot. For all immunoblot samples, cortical tissue was homogenized in RIPA buffer and centrifuged at 15,000 rpm for 15 minutes at 4°C to isolate proteins, and protein concentration was determined using the Pierce BCA Protein Assay Kit (Thermo Scientific, Rockford, IL). Twenty-five µg of protein was run on SDS polyacrylamide gel electrophoresis and transferred onto nitrocellulose membrane (n=6-10/group). The blots were probed with antibodies against cyclin-dependent kinase (CDK) 4 (1:2000, Santa Cruz Biotechnology, Inc., Santa Cruz, CA), Iba-1 (1:2000, Wako Chemicals, Richmond, VA), and proliferating cell nuclear antigen (PCNA) (1:2000, Santa Cruz Biotechnology Inc., Santa Cruz, CA); GAPDH (1:2000; Sigma-Aldrich) was used as an endogenous control. Immune complexes were detected with the appropriate HRP-conjugated secondary antibodies (KPL, Inc., Gaithersburg, MD) and visualized using SuperSignal West Dura Extended Duration Substrate

(Thermo Scientific). Chemiluminescence was captured on a Kodak Image Station 4000R station (Carestream Health), and protein bands were quantified by densitometric analysis using Carestream molecular imaging software. The data presented reflect the intensity of the target protein band compared to the control and were normalized based on the intensity of the endogenous control for each sample.

5.0 RESULTS

5.1 Statement of Work Technical Requirements

5.1.1 Determine How the Timing of AE/HB Affects Different Forms of Combat-Associated TBI. Deliverables include the following:

1. Determine whether exposure to HB after TBI caused by either fluid percussion or acceleration significantly affects histopathology or behavior.
2. Determine the optimum "time-to-fly" after TBI through comparison of outcomes after early, standard, and delayed exposure to HB.
   Approach: *The effects of exposure to AE-relevant HB were tested using both the underbody blast TBI model and the lateral fluid percussion (LFP) TBI model using rats of the same sex (male), strain (Sprague-Dawley), and size (250 – 350 g). Rats were exposed for 6 hours to HB (=8,000 feet), starting at 6 hours, 24 hours, 72 hours, or 7 days after TBI. Primary histologic and neurologic outcomes were measured up to 30 days later.*
3. Determine whether two exposures to HB after TBI worsen any outcomes compared to those observed with primary HB alone.
   Approach: *To simulate the effects of an initial flight from, for example, Afghanistan to Germany followed by a second flight from Germany to the United States, we exposed rats from each TBI group to 6 hours of HB starting at 24 hours post-TBI, followed by a second 6- or 10-hour exposure starting at 72 hours post-TBI. Primary histologic and neurologic outcomes were measured up to 30 days later.*

5.1.1.1 Histopathology

5.1.1.1.1 Effects of HB after Blast TBI

Cell Death and Axonal Injury. Prior to the start of this project, we used Fluoro-Jade B staining to probe for cell death in the cortex and hippocampus of rats at 7-30 days following TBI induced by blast-induced acceleration of 50-100 G. Despite our success with this probe in other rodent TBI models, we found no evidence for cell death in the brains of blast TBI animals compared to the extremely minor background observed in the ketamine-anesthetized sham animals [2]. Considering the fact that diffuse axonal injury is also apparent in a variety of different rodent TBI models, we tested for this in our underbody blast model using the de Olmos silver staining method. Figure 1 describes this technique and provides an example of the staining observed at 7 days post-injury. Figure 2 provides the quantification of silver staining in the internal capsule in shams that were ketamine anesthetized but not exposed to the blast and in rats subjected to 100-G force acceleration in the absence of subsequent exposure to HB or in the

presence of 6 hours HB exposure initiated at 6 hours, 24 hours, 72 hours, or 6 days post-blast. There was a small but significant increase in silver staining following blast alone and following blast plus exposure to HB at any of these times. Most importantly, the axonopathy was worse following blast plus any of the HB exposure times compared to blast and no HB.

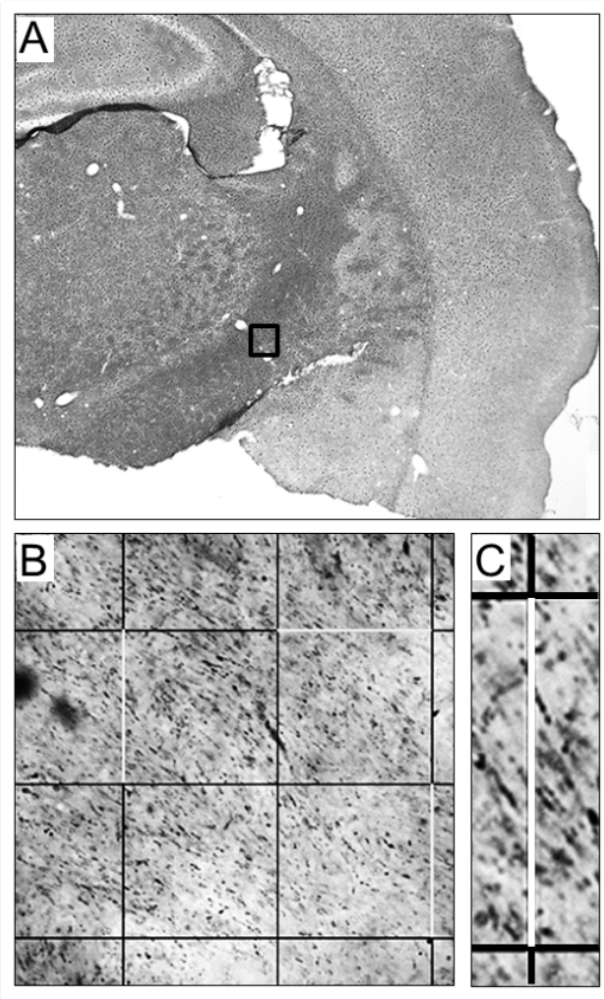

Figure 1. Quantification of amino cupric silver-stained axons at 7 days post-underbody blast injury. *Bregma level -2.30 and location within the internal capsule body were first located under low magnification (A). A 25- x 2- µm grid overlay was then placed over the reference point under 100x magnification using Stereo Investigator software (B). The number of silver-stained axons crossing 5 random 25-µm lines (C) within a given field of view was then counted throughout the 40-µm-thick section to yield a total number of axonal crossings per 5,000 µm^2.*

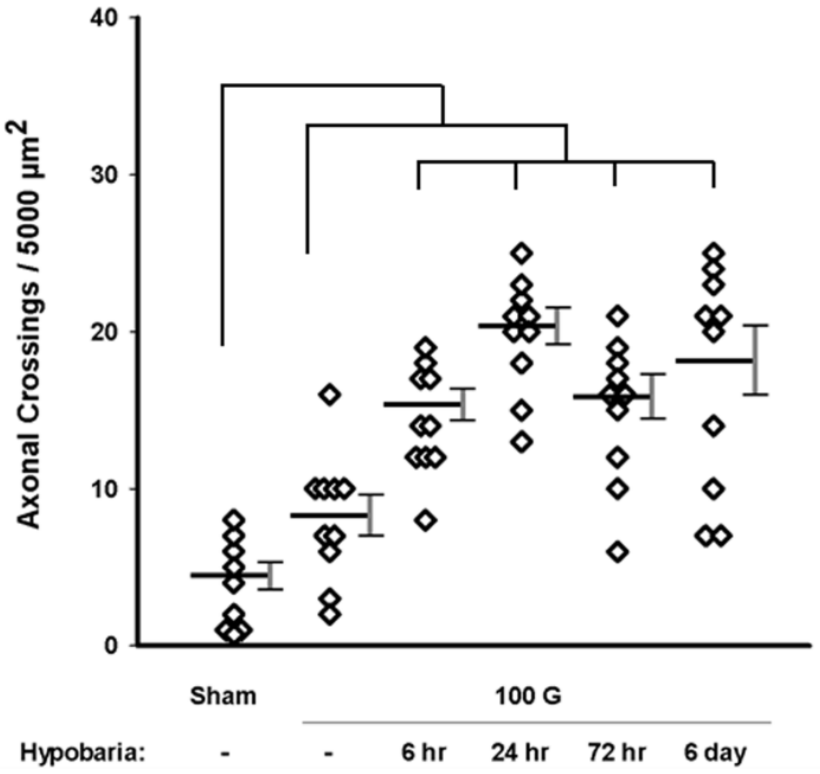

Figure 2. Hypobaria increases the number of silver-stained axonal fibers present in the internal capsule at 7 days after underbody blast induced TBI. *All 100-G blast TBI groups exposed to HB are significantly greater than TBI alone (n=9-10/group; p<0.05). All 100-G blast TBI groups are significantly greater than shams (n=9-10/group; p<0.05). Number of axonal crossings present in the 24-hour group is greater than either the 6-hour or 72-hour HB group (p<0.05).*

We then performed experiments simulating a scenario where the initial AE occurred at 24 hours after TBI and then a second AE occurred at 72 hours post-injury. As shown in Figure 3, the internal capsule silver staining following two 6-hour exposures to HB was not greater than the staining observed following single exposures at 24 or 72 hours.

Blood Brain Barrier Disruption. Cerebrovascular injury often occurs in rodent TBI models. We therefore performed immunohistochemistry for IgG to determine if leakage of this macromolecule from the blood vessels into the brain parenchyma occurs following underbody blast TBI. As shown in Figure 4, IgG leakage following 100-G blast alone was not greater than shams; however, IgG effusions were larger in rats following blast and subsequent exposure to HB at 24 hours compared to shams. Two flights did not increase IgG effusion compared to one flight at either 24 or 72 hours.

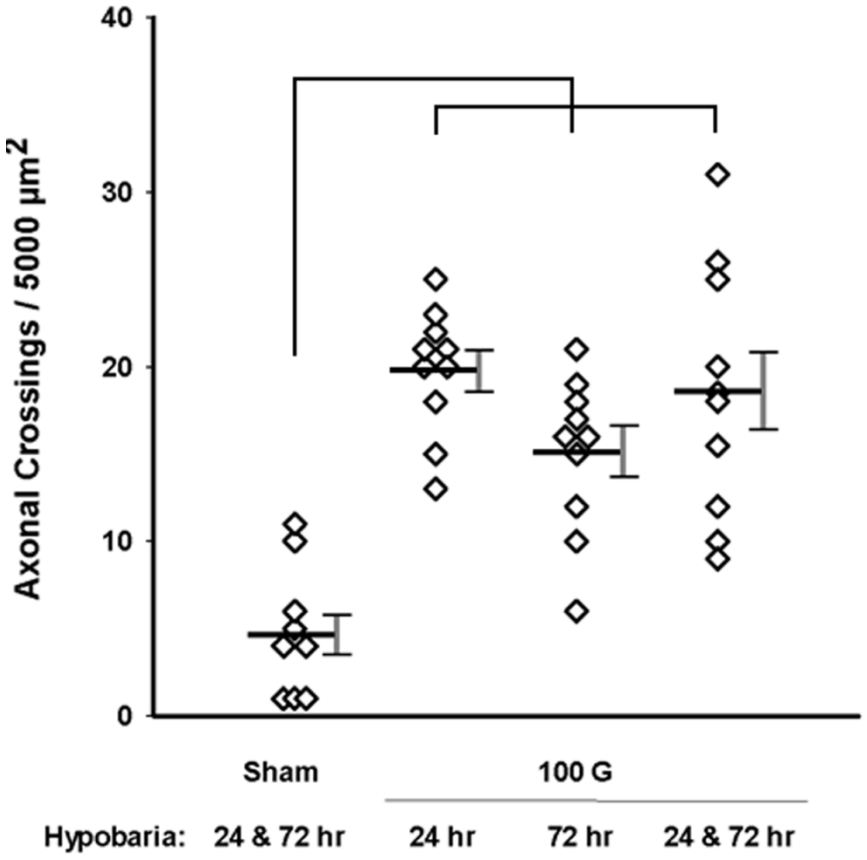

Figure 3. Exposure to a second, delayed HB does not exacerbate axonal injury induced by a single HB exposure in the internal capsule at 7 days after underbody blast injury. *All 100-G blast TBI groups exposed to single or double HB have significantly greater axonal injury than shams (n=9-10/group; p<0.001). There are no differences in number of injured axons between single or double HB exposed groups following TBI.*

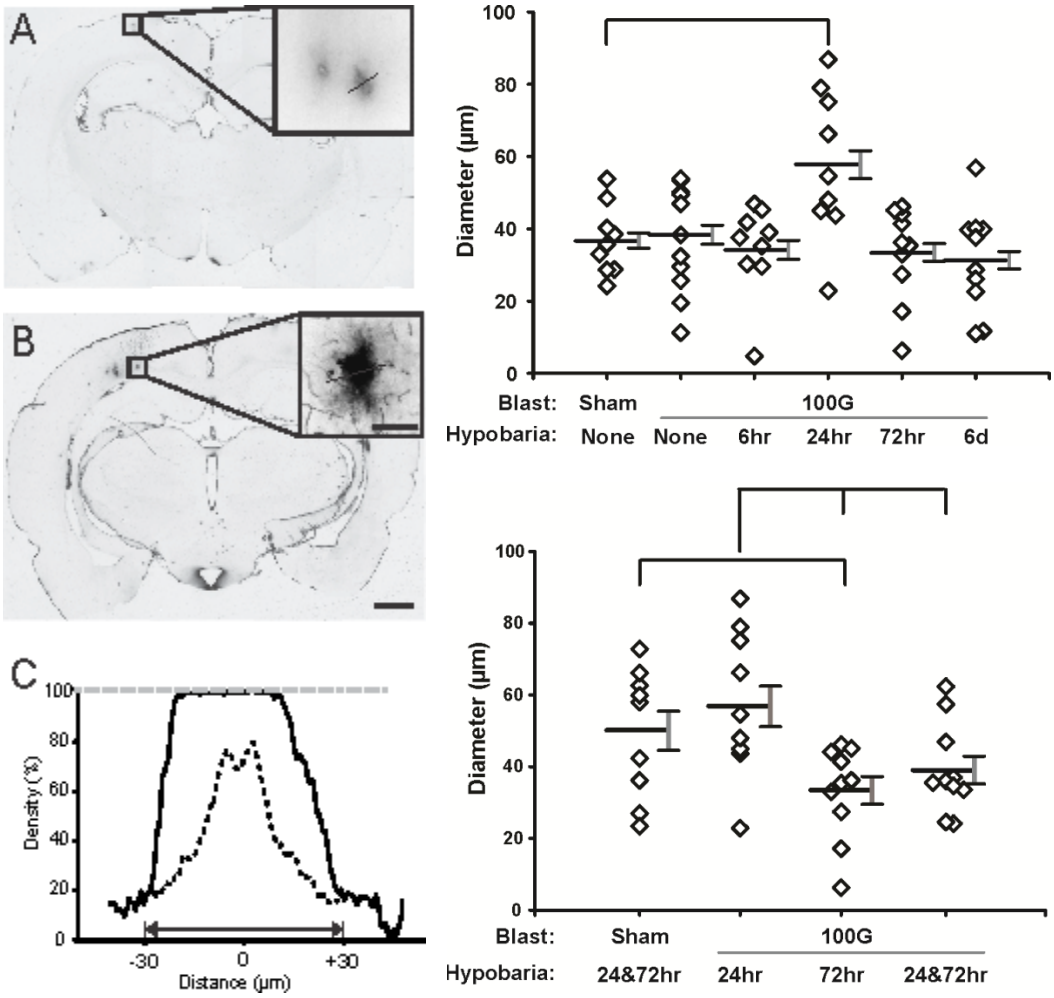

Figure 4. IgG effusions in rat cortex 7 days following 100-G blast. *Representative whole rat brain sections of sham in (A) and 100-G blast in (B). Scale bar = 500 µm. The effusion diameters were measured as in (C). The mean IgG effusion diameter was significantly greater than shams in the brains of only rats subjected to blast and HB at 24 hours ($p<0.05$). Rats that were exposed to "two flights" exhibited lower IgG effusion than those flown only at 24 hours ($p<0.05$).*

5.1.1.1.2 Effects of HB after LFP TBI

Hippocampal Neuronal Death. The LFP model also generates diffuse axonal injury; however, unlike the underbody blast model, the LFP model results in considerable death of cortical and hippocampal neurons. Figure 5 provides representative images of cresyl violet-stained brain sections illustrating neuronal cells in the CA3 subregion of the hippocampus at 30 days post-HB in sham, TBI no HB, and TBI + HB initiated at 6 hours post-injury. Figure 5 also provides quantification of the neuronal cell bodies present in the CA1, CA2/3, and dentate gyrus subregions as well as the total number of hippocampal neurons. In each of these regions, there was a significant, 10-20% loss of neurons 30 days following LFP alone. Neuronal death following exposure to HB at 6, 24, or 72 hours was significantly greater than in the absence of HB. Additional measurements were made of cortical lesion volume. There were no significant differences in lesion volume between rats that underwent LFP alone compared to those that were exposed to HB at either 6, 24, or 72 hours after the injury.

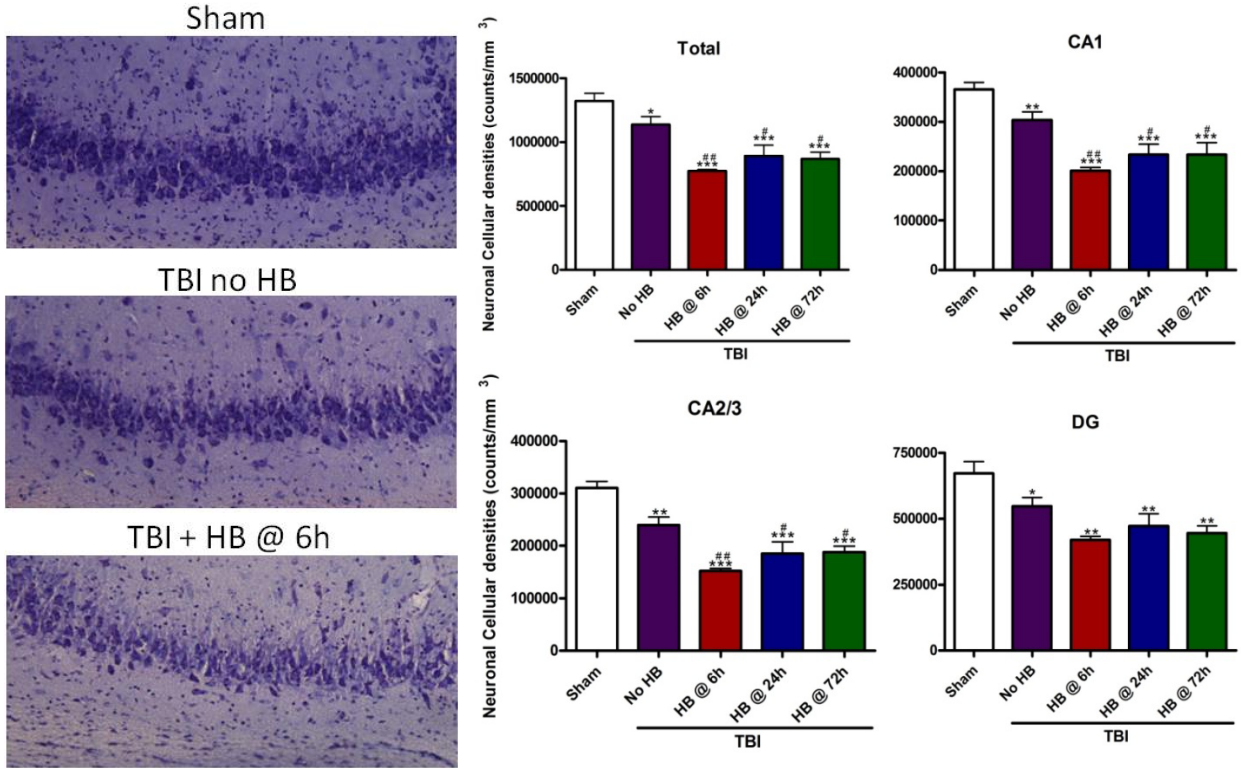

Figure 5. Hypobaria following TBI increases neuronal cell loss in the hippocampus. *Total neuronal cell numbers in the hippocampus ipsilateral to the site of injury were evaluated at post-HB day 30 using unbiased stereological quantification. TBI caused significant neuronal cell loss in the CA1 and CA2/3 subregions of the hippocampus and the dentate gyrus vs. the sham injury group (*p<0.05, **p<0.01, ***p<0.001, TBI no HB vs. sham injury; one-way analysis of variance (ANOVA) followed by Student-Newman-Keuls post hoc test). Hypobaria exposure following TBI significantly increased hippocampal cell loss in the CA1 and CA2/3 subregions vs. the TBI no HB group ($^{\#}p<0.05$, $^{\#\#}p<0.01$, HB @ 6, 24, or 72 hours vs. TBI no HB; one-way ANOVA followed by Student-Newman-Keuls post hoc test).*

Effect of HB on Microglial Activation. Dr. Faden and his colleagues have been leaders in research directed at understanding the roles of acute and chronic cellular inflammatory reactions in long-term outcomes following TBI. Since it is well established that microglial activation occurs within hours after TBI, we hypothesized that exposure of rats to HB within hours to days after LFP TBI would exacerbate this form of neuroinflammation. Figure 6 provides examples of changes in microglial morphology during activation that include an increase in the size of the cell bodies and a reduction in ramified microglial processes. Stereologic quantification of resting, activated, and total microglia present in the injured cortical hemisphere was conducted on brains perfusion-fixed at 30 days ± exposure to HB. No significant changes in microglial number or activation occurred following LFP alone compared with uninjured shams. However, both activated and total microglia were greater in rats following exposure to 6 hours of HB initiated at 6, 24, or 72 hours compared with shams and compared with injury and no exposure to HB. There was no change in the number of resting microglia, indicating that most of the activated microglia arose by cell proliferation. Similar results were observed under the same conditions when brains

were perfusion-fixed at 7 days following injury. Thus, early exposure to HB exacerbates both early and chronic neuroinflammation. *A more complete description of these and other results obtained with the LFP TBI model is included in Skovira et al. [6].*

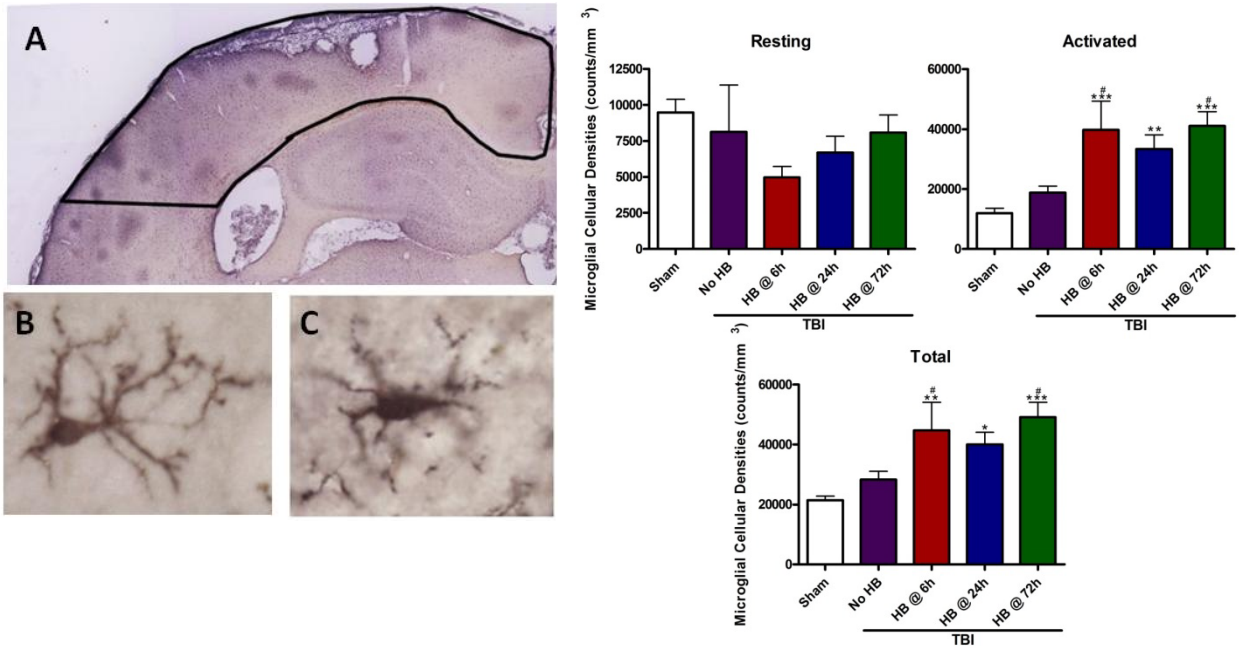

Figure 6. Quantification of microglial cell numbers in the injured cortex 30 days post-HB. *Morphological phenotypes of microglia for unbiased stereological quantifications of microglial cell numbers in the injured cortex (A) were used to differentiate between resting (B) and activated states (C). Unbiased stereological quantification based on morphological appearance of microglia in the ipsilateral cortex (resting state, activated state, and total). At 30 days post-HB, the number of activated and total microglia was significantly increased in TBI + HB @ 6, 24, or 72 hours vs. the sham injury group and in the TBI + HB @ 6 or 72 hours vs. the TBI no HB group (***p<0.001, **p<0.01, *p<0.05 vs. sham injury; #p<0.05 vs. injured no HB; one-way ANOVA followed by Student-Newman-Keuls post hoc test).*

5.1.1.2 Neurobehavioral Outcomes

5.1.1.2.1 Effects of HB on Neurologic Outcome after Blast TBI. The following tests were performed on rats at up to 7 days following blast TBI in the absence and presence of exposure to HB under room air at 24 hours post-blast: composite neuroscore, novel object recognition, beam walking (latency and foot faults), and open field (distance, immobility, rearing, grooming, center entries). We also performed these tests on rats that were "flown" twice, i.e., at 24 and 72 hours. There were no significant differences in any of these outcome measures comparing any of the blast TBI ± HB groups with shams. As described later, neurobehavioral abnormalities were detected when we compared shams with blast TBI animals that were exposed to 6 hours of HB under 100% O_2 at 24 hours post-blast. The lack pf neurobehavioral changes observed with this model is due to two factors. First, the 100-G level of acceleration is relatively low compared to the up to 2,800-G accelerations that we subsequently found were both survivable and that resulted in significant behavioral alterations. Second, the fact that little if any neuronal cell death occurs in this model, at least at relatively low G levels, reduces the odds of detecting neurologic

alterations by routine methods. Thus, the effects of HB on behavior were expected to be more robust using the LFP moderate TBI injury model that is associated with both diffuse axonal injury and cortical and neuronal death.

5.1.1.2.2 Effects of HB on Neurologic Outcome after LFP TBI. The MWM was used to evaluate whether primary AE or primary plus secondary AE following brain injury causes increased deficits in spatial learning in comparison to shams. No significant learning deficits were observed in the acquisition phase of MWM following exposure to HB at 24 hours after LFP. Spatial memory was assessed using the MWM probe trial on day 18 post-HB by examining the time spent in the target quadrant following removal of the platform (Figure 7). TBI plus HB exposure vs. primary AE and secondary AE exposure animals demonstrated a significant impairment in spatial memory in primary AE and secondary AE exposed animals. Swim speeds did not differ between animals exposed to a single AE equivalent (TBI + HB) and the primary and secondary HB exposure group.

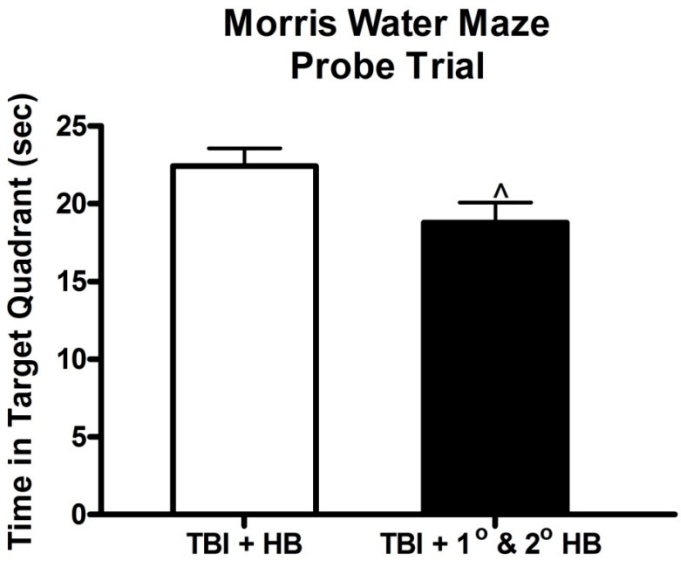

Figure 7. MWM probe trial time in target quadrant following primary and secondary HB. *Spatial memory was assessed using the MWM probe trial on day 18 post-HB by examining the time spent in the target quadrant following removal of the platform. TBI plus HB exposure vs. the primary and secondary HB exposure group demonstrated a significantly greater impairment in spatial memory following two HB exposures (^p<0.05; one-tailed t-test).*

Non-spatial memory was assessed by the novel object recognition test on post-HB day 21 to evaluate if two HB exposures increased non-hippocampal dependent memory deficits in comparison to a single HB exposure (Figure 8). During the testing phase, the primary AE and secondary AE exposed animals exhibited a significant decrease in the discrimination index from that of TBI + HB exposed animals.

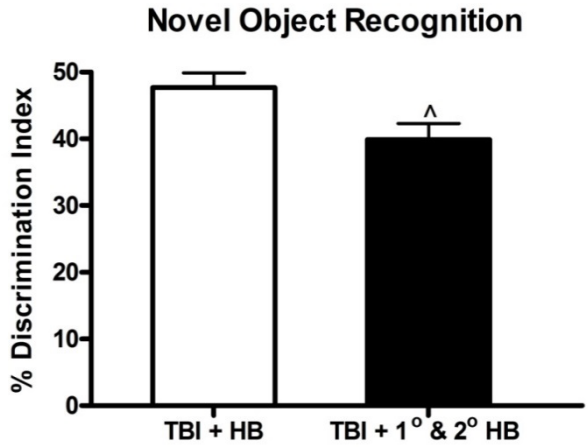

Figure 8. Novel object recognition following primary and secondary HB. *Non-spatial memory was assessed by a novel object recognition test on post-HB day 21. During the testing phase, the primary and secondary HB exposure group showed a significant decrease in the discrimination index in comparison to TBI + HB exposed animals (^p<0.05; one-tailed t-test).*

5.1.2 Develop Potential Therapeutic Strategies to Limit AE-Induced Inflammation and Cerebral Metabolic Impairment and to Improve Neurologic Outcome

5.1.2.1 Effects of Hyperoxia during HB Following TBI. The question of how different levels of inspired oxygen during AE could affect TBI outcomes was raised during discussions with Colonels Raymond Fang and Stacey Shackelford at C-STARS Baltimore. They indicated that any patient transported following severe TBI or who was ventilated would likely receive levels of oxygen in the 70-100% range. Patients with mild TBI would also receive supplemental oxygen in the 30-50% range. We therefore tested the effects of different inspired oxygen levels during exposure to HB subsequent histologic and neurologic outcomes, using both the mild blast TBI model and the moderate LFP TBI model. *A more complete description of these and other results obtained with the LFP TBI model is included in Skovira et al. [6]*.

5.1.2.1.1 Effects of Hyperoxia during AE after Blast TBI

Axonal Injury. In these experiments, we compared the average number of silver-stained neurons in the internal capsule at 7 days post-blast, present in shams, TBI + HB under 21% O_2, and TBI + HB under 100% O_2. A 6-hour period of HB was initiated at 24 hours post-blast. We found a significant increase in either TBI + HB group compared to shams (Figure 9). We also found that the number of damaged neurons was greater in animals exposed to 100% O_2 during HB compared with those exposed to 21% O_2 during HB.

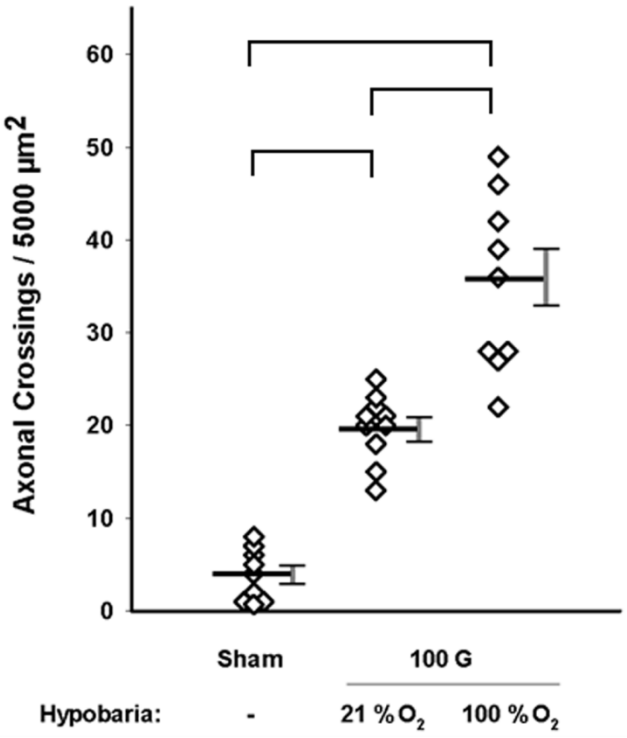

Figure 9. Hyperoxia during HB exacerbates axonal injury present in the internal capsule with normoxic HB exposure at 7 days after underbody blast. *Both 100-G blast TBI groups exposed to 21% or 100% inspired O_2 during HB have significantly more injured neurons than shams (n=9-10/group; p<0.001). The number of axonal crossings present in the 100% O_2 group is greater than in the 21% O_2 hypobaric group (p<0.001).*

Blood Brain Barrier Disruption. We also compared the diameter of perivascular IgG effusions present in the rat cortex at 7 days following sham anesthesia, blast TBI + HB under 21% O_2, and TBI + HB under 100% O_2 (Figure 10). Hypobaria was initiated at 24 hours post-blast. In these experiments, we found that the IgG effusions were larger in animals exposed to HB under 21% O_2 but not 100% O_2 compared to shams.

von Willebrand Factor (vWF) Immunoreactivity. Considering the IgG immunohistochemical data indicating a disruption of the cerebral cortex blood brain barrier after blast TBI, we performed immunohistochemical measurements of vWF, which often increases in the cerebral vasculature following injury. As shown in Figure 11, vWF immunostaining was abundant and localized primarily to blood vessels in the cortex of an animal exposed to blast TBI and then to HB under 21% O_2. Immunostaining in a ketamine-anesthetized sham rat was very scarce. Immunostaining area as a percentage of total area analyzed was less than 1% for shams and 3-9% for blast TBI + HB. There was no significant difference, however, in the area of staining for blast TBI animals exposed to HB under 21% O_2 compared with those exposed to 100% O_2.

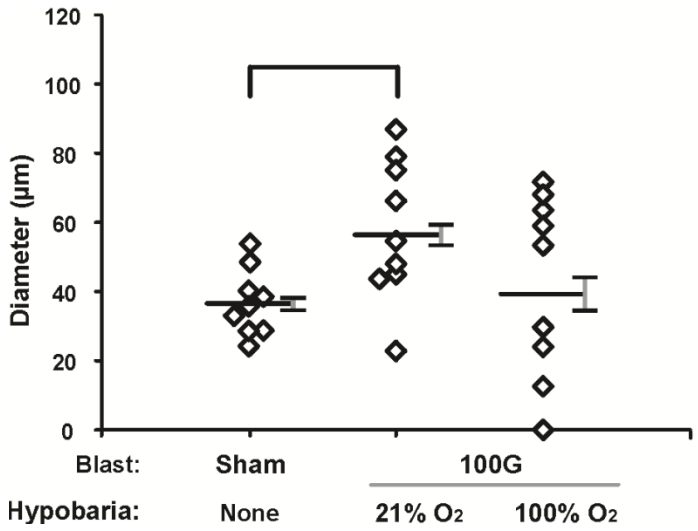

Figure 10. Effect of oxygen level during HB on IgG effusions at 7 days post-blast. *Animals were exposed to 6 hours of HB under either 21% or 100% O_2. The mean IgG effusion diameter was greater in animals exposed to HB under 21% O_2 but not 100% O_2 compared to shams ($p<0.05$).*

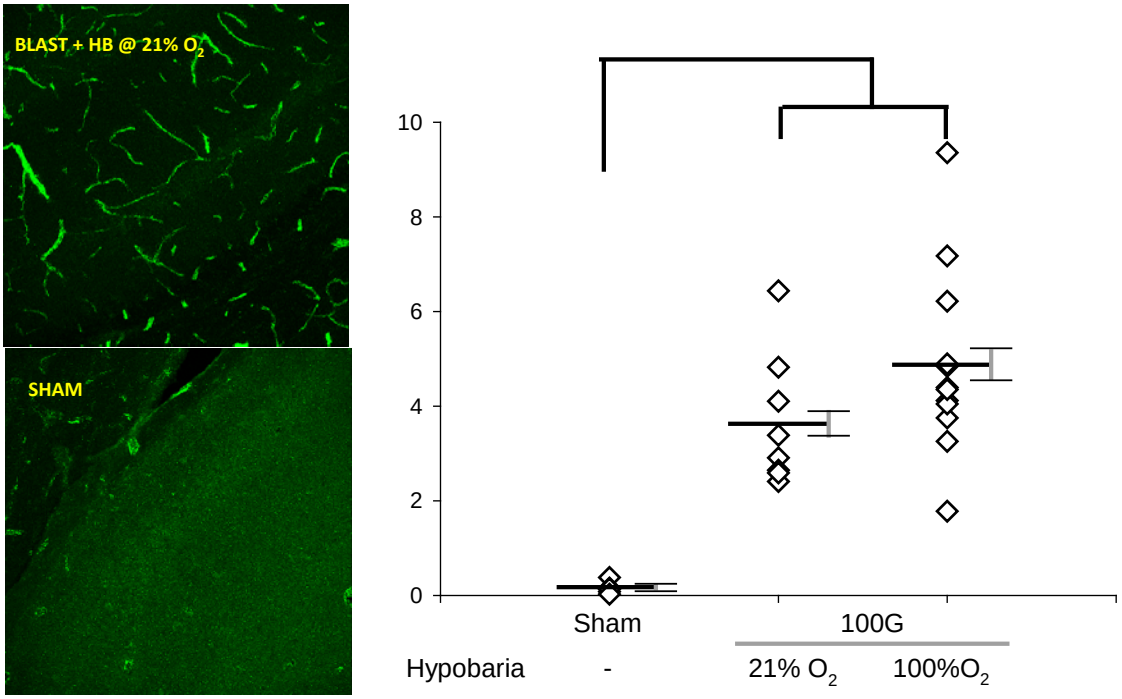

Figure 11. vWF immunoreactivity in the cortex 7 days post-blast and subsequent exposure to 6 hours of HB initiated at 24 hours post-blast under 21% or 100% O_2. *vWF immunoreactivity is scarce in shams but abundant in the cortex or rats following blast TBI and exposure to HB. The area of vWF immunoreactivity for blast TBI + HB at either oxygen level was significantly greater than shams ($p<0.01$) but there was no difference between animals exposed to 21% vs. 100% O_2 during HB.*

Neurobehavioral Measurements. Even though we did not observe differences in behavior comparing sham rats with those exposed to HB under 21% O_2, we performed additional behavioral assays to determine if any abnormalities were apparent in rats exposed to HB under 100% O_2. All of these experiments employed a 6-hour HB exposure initiated at 24 hours following exposure of rats to ketamine-anesthesia (shams) or to anesthesia followed immediately by exposure to a 100-G underbody blast. No differences were observed in the number of foot faults among rats in the three groups at baseline, measured 24 hours prior to blast or sham anesthesia. No differences were observed when the number of foot faults at baseline was compared with those at 7 days post-blast for shams or HB under 21% O_2. The number of foot faults for blast TBI rats exposed to HB under 100% O_2 was both significantly greater than baseline and greater than the number following HB under 21% O_2 (Figure 12). Additional measurements of latency to cross the beam detected no effects of blast under either HB condition (not shown).

Other tests that were performed include composite neuroscore, open field, and novel object recognition. No significant differences were observed among shams, blast + HB at 21% O_2, and blast + HB at 100% O_2.

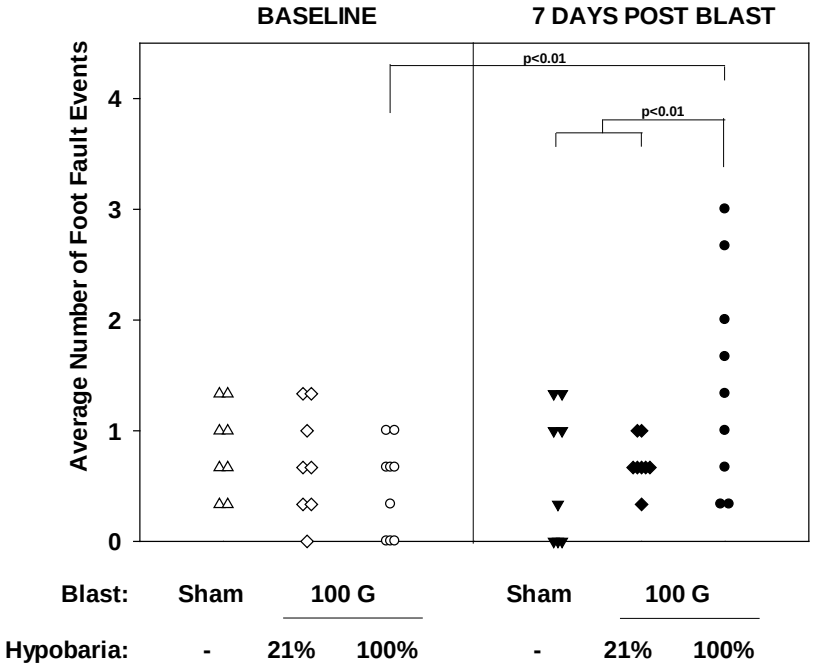

Figure 12. Exposure to hyperoxia during HB following blast TBI increases foot faults during the balance beam test. *All tests were conducted 24 hours prior to blast exposure (baseline) and at 7 days post-blast. Repeated measures two-way ANOVA detected a difference in blast + HB under 100% O_2 compared to shams and blast + HB under 21% O_2 (n=8-9/group).*

5.1.2.1.2 Effects of Hyperoxia during AE after LFP TBI

Effects of Hyperoxia on Neurobehavioral Outcome Measures. All animals used in these experiments were subjected to LFP TBI and then exposed to the standard HB level for 6 hours beginning at 24 hours following injury. Animals randomized to the groups used in these comparisons following LFP TBI were slightly different from those used with the blast TBI model. Specifically, the "normoxic" group was exposed to HB under either 28% or 100% O_2. The rationale for using 28% rather than the standard 21% level used following blast-induced mild TBI was that most, if not all, AE patients who suffer from a moderate TBI level are provided with supplemental oxygen at a level of at least 28%, which at 8,000 feet cabin pressure results in an effective oxygen level of 21%. If intubated, the vast majority of moderate to severe TBI patients would be ventilated on 100% O_2.

Tests determining the latency to reach the submerged platform in the MWM test acquisition phase indicated no significant difference between LFP + HB rats exposed to 28% or 100% O_2 during HB (not shown). However, the search strategies used to reach the platform were significantly different between these groups (Figure 13). Animals exposed to hyperoxia during HB displayed an insignificant trend toward utilizing less of a spatial search strategy than the TBI + HB group and relied primarily on a systematic search strategy.

Following the acquisition phase, the two animal groups were tested for spatial memory by measuring the time spent in the correct quadrant of the water maze during the probe trial at 18 days post-HB. The hyperoxia group demonstrated a significant impairment in spatial memory in comparison to TBI + HB under 28% O_2 group (Figure 14).

The normoxic and hyperoxic HB groups were also compared using the forced swim test on day 26 post-HB for anxiety and depression. The results shown in Figure 15 indicate that rats exposed to HB under 100% O_2 spent significantly more time immobile in the water cylinder than the rats exposed to 28% O_2 during HB.

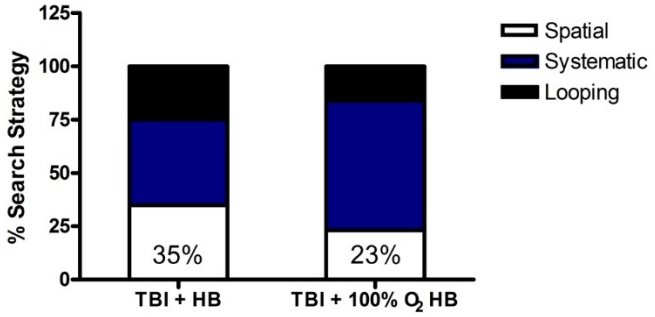

Figure 13. Morris water maze acquisition search strategy at day 4 following LFP and HP. *The swimming patterns during all trials on the fourth day of the acquisition phase were analyzed to assess the search strategies utilized by the animals to locate the hidden platform. A chi-square analysis was used to compare strategies across groups and was found to be significant ($p< 0.0121$, $\chi 2 =8.825$, $df=2$).*

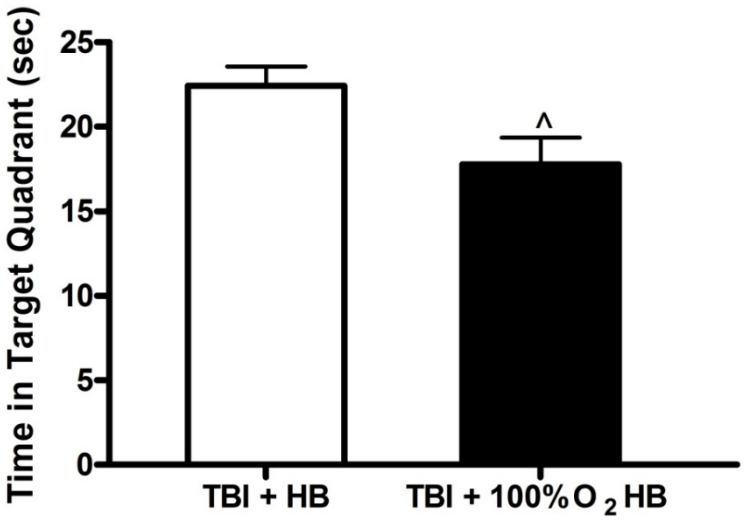

Figure 14. Effects of hyperoxia during HB following TBI on depressive-like behaviors. *Spatial memory was assessed using the MWM probe trial on day 18 post-HB by examining the time spent in the target quadrant following removal of the platform (^p<0.05; one-tailed t-test).*

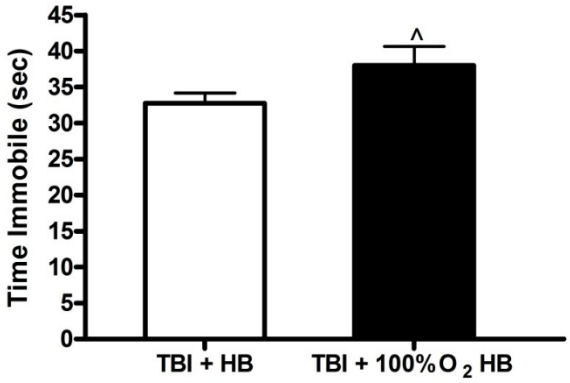

Figure 15. Effects of hyperoxia during HB following TBI on depressive-like behaviors. *Hyperoxia during HB significantly increased depressive-like behavior in comparison to the TBI + HB group (^p<0.05; one-tailed t-test).*

5.1.2.2 Inhibition of Neuroinflammation and Neuroprotection by a Cyclin-Dependent Kinase Inhibitor

5.1.2.2.1 Change in Approach from Original Statement of Work. The original Statement of Work indicated that our approach to this deliverable would be to use an advanced inhibitor of the enzyme poly-ADP-ribose polymerase (PARP), which is important in triggering neuroinflammation. However, due in part to the outstanding inhibition of inflammation that Dr. Faden's lab demonstrated with a CDK inhibitor (CR8) in another TBI paradigm, the Air Force agreed to substitute CR8 for the PARP inhibitor.

5.1.2.2.2 Effects of HB and CR8 on Inflammation Biomarkers. Early assays of inflammatory cytokines in the serum of rats subjected to LFP TBI indicated that there was no increase at 24 hours after injury in the absence of exposure to HB under 28% O_2 (not shown). There were also no differences in the levels of inflammatory cytokines in the ipsilateral cortex of LFP rats not exposed to HB compared to shams. However, the level of brain IL-6 (pro-inflammatory) and IL-10 (anti-inflammatory) was significantly higher in rats exposed to 6 hours HB compared to shams (Table 1). To examine whether HB exposure following injury increased markers of microglial activation and cell cycle activation, Western blotting was performed for the inflammatory microglial marker IBA-1 and proliferating cell markers PCNA and CDK4 (Figure 16). At 24 hours post-injury, a significant increase in the protein expression of all three markers was observed in the injured no HB exposure group in comparison to the sham injury group. Hypobaria exposure following TBI significantly increased the protein expression of all three markers in comparison to the TBI no HB exposure group.

Table 1. Prolonged HB Following TBI on Cerebral Cytokine Levels (pg/mg protein)

Cytokine	Sham	TBI No HB	TBI + HB
IL-1β	16,446 (±3,163)	37,485 (±13,380)	42,840 (±10,321)
IL-2	1,093 (±211)	1,238 (±216)	1,605 (±248)
IL-6	2,473 (±314)	4,599 (±767)	6,309 (±1,212)[a]
IL-10	476 (±162)	567 (±123)	1,785 (±340)[b]
IL-12	1,293 (±265)	3,884 (±1,503)	4,919 (±1,317)
IFN-γ	3,089 (±146)	3,874 (±406)	4,490 (±500)

Note: Cytokine levels in the ipsilateral cortex were assayed at 24 hours post-injury using a using a multiplex ELISA (Q-Plex™, Quansys Biosciences). One-way ANOVA followed by Student-Newman-Keuls *post hoc* test for all analyses.

[a]Levels of IL-6 were significantly elevated in the TBI + HB group in comparison to sham injury ($p<0.05$).

[b]IL-10 was significantly elevated in the TBI + HB group in comparison to the sham injury group ($p<0.05$) and TBI no HB group ($p<0.05$).

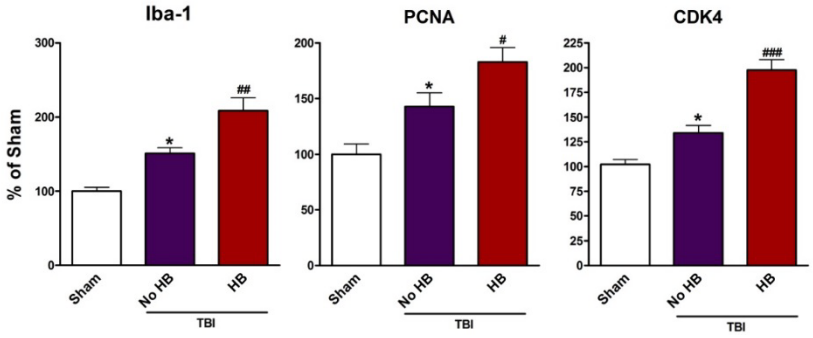

Figure 16. Hypobaria exposure increases markers of microglial and cell cycle activation. *At 24 hours post-injury, a significant increase in the protein expression of Iba-1, PCNA, and CDK4 was observed in the TBI no HB exposure group in comparison to the sham injury group (*p<0.05 TBI no HB vs. sham injury; one-way ANOVA followed by Student-Newman-Keuls post hoc test.) Hypobaria exposure following TBI significantly increased the protein expression of all three markers in comparison to the TBI no HB exposure group (#p<0.05, ##p<0.01, ###p<0.001 TBI + HB vs. TBI no HB; one-way ANOVA followed by Student-Newman-Keuls post hoc test).*

Increasing evidence indicates that circulating MPs (or microvesicles) contribute to systemic inflammation in a number of pro-inflammatory pathologies, including rheumatoid arthritis. These particles can arise from a wide variety of cells including platelets, endothelial cells, microglia, and neurons. To determine if HB exposure following TBI influenced levels of circulating MPs, the absolute number of MPs per milliliter in serum samples was analyzed using flow cytometry (Figure 17). There was no significant difference found between groups (n=6-10/group; p=0.2347; one-way ANOVA followed by Student-Newman-Keuls *post hoc* test). Hypobaria exposure displayed a non-significant trend toward increased levels of circulating MPs in comparison to the TBI no HB group.

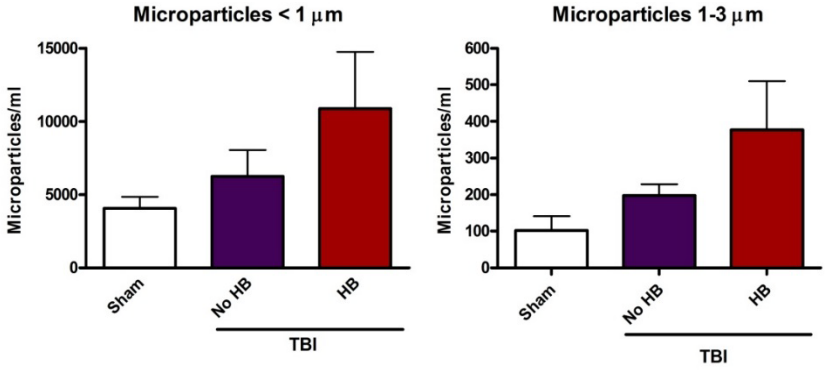

Figure 17. Effects of HB following TBI on levels of circulating MPs. *The absolute number of MPs per milliliter in serum samples was analyzed using flow cytometry. There was no significant difference found between groups (p=0.2347; one-way ANOVA followed by Student-Newman-Keuls post hoc test). HB exposure displayed a non-significant trend toward increased levels of circulating MPs in comparison to the TBI no HB group.*

Evidence that inflammation plays a role in the exacerbation of TBI caused by exposure to HB came from experiments where rats were administered CR8, a potent second-generation CDK inhibitor. The Faden lab previously published evidence that CR8 inhibits activation of microglia and astrocytes and improves neurologic outcome following TBI in the absence of exposure to HB [5,7]. To evaluate if CR8 modulates the early neuroinflammatory response following TBI + HB, cytokine levels were assayed at 24 hours post-injury using a multiplex ELISA (n=6-10/group). IL-2, IL-10, and IL-12 were the only cytokines that were detected in plasma 24 hours post-injury, and levels of these cytokines were not further influenced by CR8 treatment following TBI + HB in comparison to the TBI minus HB group (Table 2). Levels of IL-1β, IL-2, IL-10, IL-12, and IFN-γ in the ipsilateral cortex were also not influenced by CR8 treatment following TBI + HB in comparison to the TBI minus HB group. Cortical levels of IL-6 showed a treatment effect with CR8 in comparison to TBI + HB but were not significantly different.

Table 2. Effects of CR8 Treatment on Plasma and Cortex Cytokine Levels Following TBI + HB

Cytokine	Plasma (pg/mL)		Cortex (pg/mg protein)	
	TBI + HB	TBI + CR8 + HB	TBI + HB	TBI + CR8 + HB
IL-1β			42,840 (±10,321)	44,850 (±3,615)
IL-2	209 (±58)	438 (±127)	1,605 (±248)	2,145 (±289)
IL-6			6,309 (±1,212)[a]	4,817 (±370)
IL-10	235 (±43)	282 (±94)	1,785 (±340)	2,329 (±768)
IL-12	18,913 (±3,193)	23,342 (±1,016)	4,919 (±1,317)	4,071 (±268)
IFN-γ			4,490 (±500)	4,825 (±664)

[a]Levels of cortical IL-6 were significantly elevated in comparison to sham injury by HB exposure and showed a treatment effect with CR8 ($p<0.05$; one-way ANOVA followed by Student-Newman-Keuls *post hoc* test).

Despite the lack of an effect of CR8 on serum or cerebral cortex inflammatory cytokines, CR8 did reduce protein carbonylation, which is a common marker of oxidative stress that is often associated with neuroinflammation. In this assay, cortex protein extracts react with dinitrophenylhydrazine, forming a protein-dinitrophenylhydrozone adduct. Western blots were then performed using antibodies to dinitrophenylhydrozone, demonstrating the large number of carbonylated proteins present at 24 hours following TBI and subsequent exposure to HB at 24 hours following the TBI (Figure 18). Densitometric quantification of total carbonyl immunoreactivity indicated that CR8 administration significantly reduced protein carbonylation in comparison to the group that received the drug vehicle.

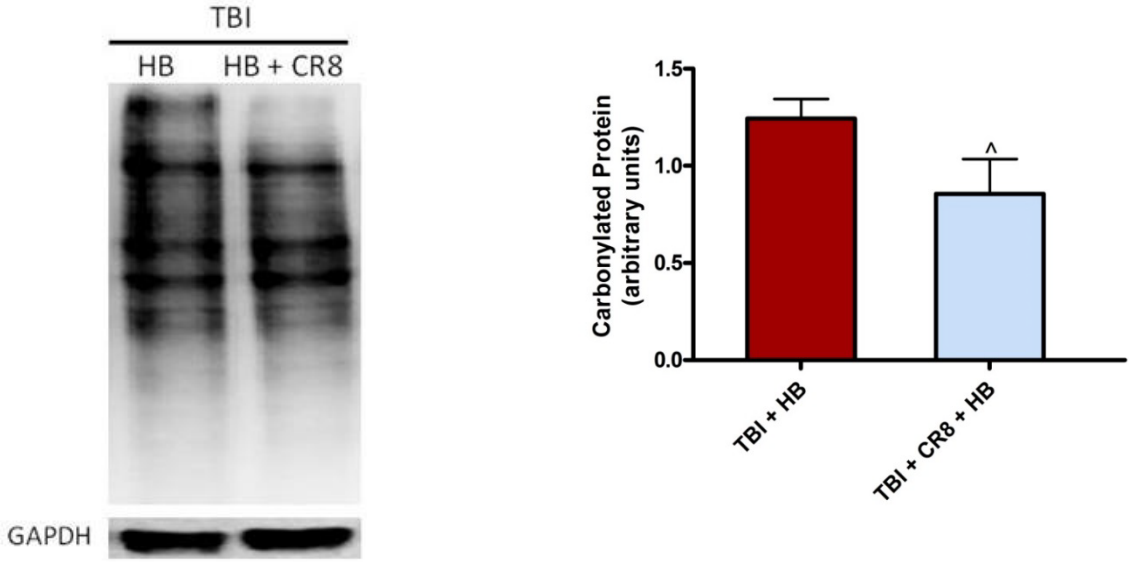

Figure 18. Effects of CR8 treatment on cerebral cortex protein carbonyl groups. *Proteins were extracted from the cerebral cortex following TBI and subsequent exposure to HB at 24 hours post-injury. Protein carbonyl groups reacted with dinitrophenylhydrazine, forming dinitrophenylhydrozone. Immunoblots against dinitrophenylhydrozone were used to quantify the level of protein carbonylation. A significant decrease in the levels of carbonylated proteins was observed in the CR8 treatment group vs. vehicle-treated animals (^$p<0.05$; one-tailed t-test).*

Immunoblot measurements were also used to determine if treatment of rats with CR8 reduces markers of microglial activation (Iba-1) and cell cycle activation (PCNA and CDK4). Figure 19 demonstrates that the levels of all three markers present following LFP TBI and exposure to HB 24 hours post-injury were approximately 100% greater than the levels observed in sham animals. Moreover, treatment of rats with CR8 significantly reduced the levels of Iba-1, PCNA, and CDK4 present following TBI plus exposure to HB.

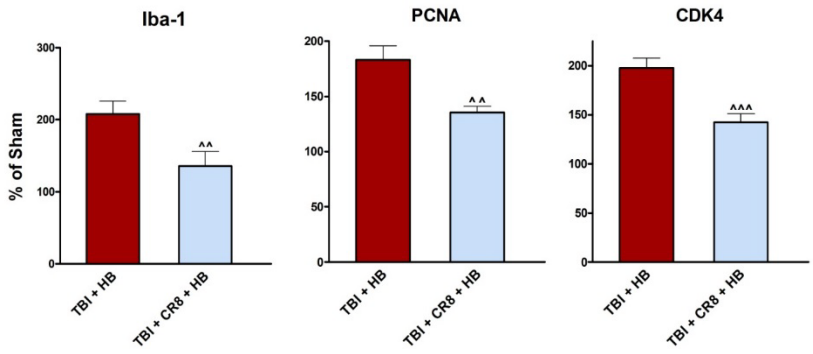

Figure 19. CR8 treatment reduces microglial and cell cycle activation marker protein levels. *Western blotting was performed for the inflammatory microglial marker Iba-1 and proliferating cell markers PCNA and CDK4. At 24 hours post-injury, a significant decrease in the protein expression of all three markers was observed in the CR8 treatment group in comparison to the TBI + HB group (^^p<0.01; ^^^p<0.001; one-tailed t-test).*

To determine if CR8 treatment also influences levels of circulating microparticles (MPs) present following TBI and HB, the absolute number of MPs per milliliter in serum samples was analyzed using flow cytometry. Figure 20 shows that CR8 treatment significantly reduced the levels of circulating MPs that are < 1 μm in comparison to the untreated TBI + HB group.

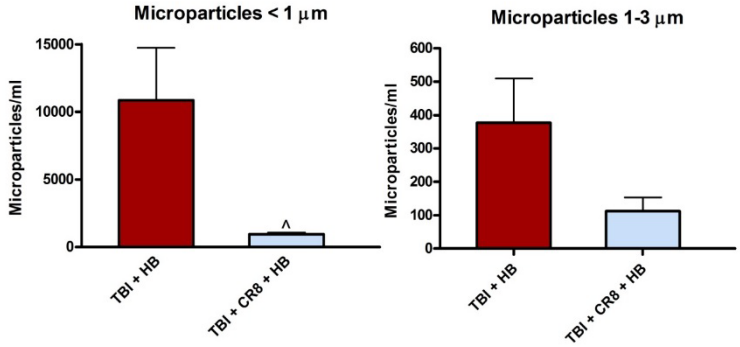

Figure 20. CR8 treatment reduces levels of circulating MPs following TBI + HB. *The absolute number of MPs per milliliter in serum samples was analyzed using flow cytometry. CR8 treatment significantly reduced the levels of circulating MPs in the size range of < 1 μm in comparison to the TBI + HB group (^p<0.05; one-tailed t-test).*

The MWM was used to evaluate if CR8 treatment attenuates deficits in spatial learning caused by HB exposure following TBI (Figure 21). Exposure of rats to 6 hours of HB starting at 6 hours post-injury induced significant deficits in spatial learning during the acquisition phase of the MWM in comparison to the sham injury group ($p<0.001$; repeated measures one-way ANOVA followed by Student-Newman-Keuls *post hoc* test). Although the TBI + CR8 + HB group exhibited significant deficits in spatial learning in comparison to the sham injury group ($p<0.001$), CR8 significantly improved spatial learning deficits in comparison to the TBI + vehicle + HB group ($p<0.01$; repeated measures one-way ANOVA followed by Student-Newman-Keuls *post hoc* test). The mean escape latency on the last day of training was 30.2 ± 3.9 seconds for the sham injured group, 68.6 ± 6.7 seconds for the vehicle + HB group, and 51.0 ± 6.7 seconds for the CR8 treated group.

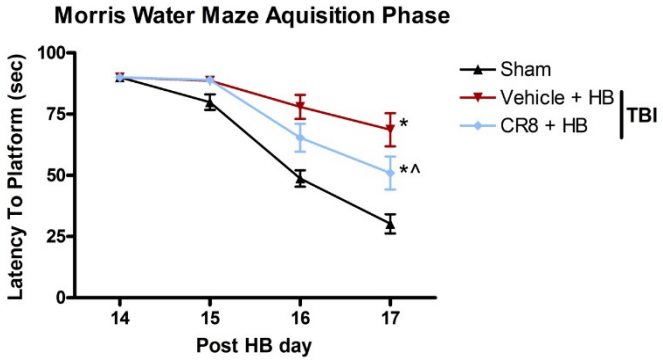

Figure 21. CR8 treatment improves cognition following TBI + HB. *The TBI + HB group showed significant deficits in spatial learning in comparison to the sham injury group (*p<0.001). CR8 treatment significantly improved spatial learning deficits in comparison to the TBI + vehicle + HB group (^p<0.01; repeated measures one-way ANOVA followed by Student-Newman-Keuls post hoc test).*

Non-spatial memory was assessed using the novel object recognition test on post-HB day 21 to evaluate if CR8 treatment improves non-hippocampal dependent memory (Figure 22). Animals showed an equal preference for the two identical objects during the training phase. During the testing phase, a significant decrease in the discrimination index was observed in the vehicle + HB group compared to the sham injury group indicating a reduced preference for the novel object ($p<0.001$ vs. sham; one-way ANOVA followed by Student-Newman-Keuls *post hoc* test). CR8 treatment significantly increased the discrimination index in comparison to the TBI + vehicle + HB group indicating an improvement in non-spatial memory ($p<0.05$ vs. TBI + vehicle + HB; one-way ANOVA followed by Student-Newman-Keuls *post hoc* test).

Total neuronal cell numbers in the hippocampus were evaluated at post-HB day 30 to determine if improvements in cognitive memory function following CR8 treatment were associated with increased hippocampal neuronal survival (Figure 23). Unbiased stereological quantifications show that moderate LFP-induced TBI + HB caused significant neuronal cell loss in the CA1 subregion of the hippocampus and the dentate gyrus vs. the sham injury group. The TBI + CR8 + HB group exhibited a non-significant trend towards sham injury neuronal levels.

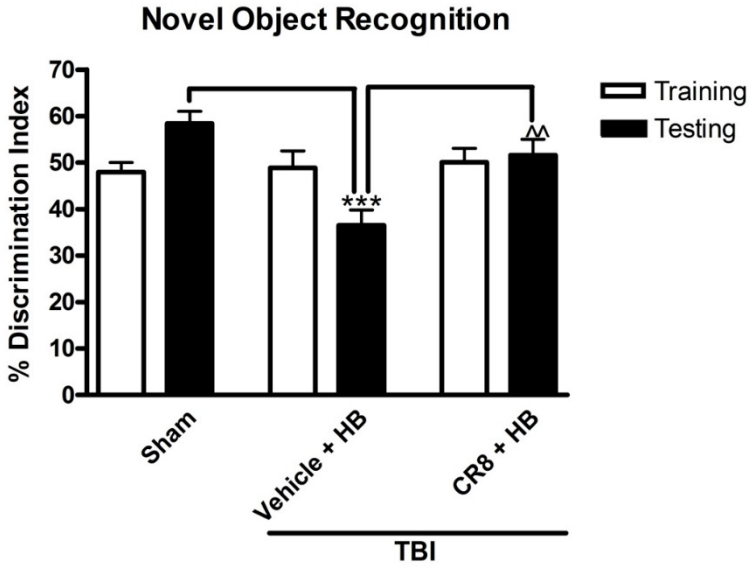

Figure 22. CR8 treatment improves non-spatial memory following TBI + HB. *Non-spatial memory was assessed using the novel object recognition test on post-HB day 21. Animals showed an equal preference for the two identical objects during the training phase. During the testing phase, a significant decrease in the discrimination index was observed in the vehicle + HB group compared to the sham injury group, indicating a reduced preference for the novel object (***p<0.001 vs. sham; one-way ANOVA followed by Student-Newman-Keuls post hoc test). CR8 treatment significantly increased the discrimination index in comparison to the TBI + vehicle + HB group, indicating an improvement in non-spatial memory (^^p<0.01 vs. TBI + vehicle + HB; one-way ANOVA followed by Student-Newman-Keuls post hoc test).*

Using unbiased stereological quantifications of resting and activated microglia cell numbers in the injured cortex were evaluated at 30 days post-HB to examine if CR8 treatment reduced the neuroinflammatory response associated with TBI + HB (Figure 23). TBI + HB exposure resulted in a significant increase in the total number of microglia and the number of activated microglia in comparison to the sham injury group. CR8 treatment significantly reduced the total number of microglia and number of activated microglia in comparison to the TBI + vehicle + HB group.

5.2 Additional Research Supported by this Project

Toward the end of this project, the research team and Dr. Vanderbeek of the 711th Human Performance Wing discussed the importance of extending the tests of AE-relevant HB using other animal models. We specifically identified polytrauma as a prime candidate, considering its military relevance and the potential sensitivity of polytrauma victims to adverse effects of HB. With Air Force approval, we performed experiments with a rat polytrauma model consisting of controlled cortical impact-induced TBI, followed immediately by 30 minutes of hemorrhagic shock when the mean arterial pressure was maintained between 35 and 40 mmHg. The rats then underwent a 1-hour “pre-hospital” resuscitation phase when pressure was near-normalized by intra-arterial infusion of the colloid Hextend. This phase was followed by a 1-hour “in-hospital” resuscitation phase when normal mean arterial pressure was fully restored by re-infusion of the blood withdrawn during the shock phase. We met the goal of these experiments, which was to

replicate the model that we used previously in another project and to prepare us for conducting a new project studying the effects of HB on survival and neurologic outcomes. Dr. Fiskum and his staff also utilized this period to finish a manuscript describing the results obtained with the previous model [8].

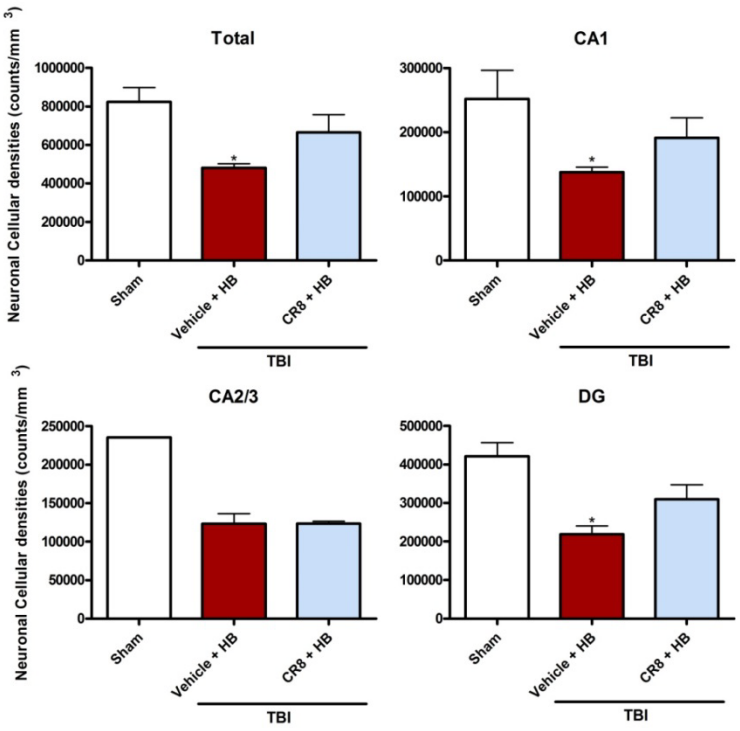

Figure 23. Effect of CR8 treatment following TBI + HB on neuronal cell loss in the hippocampus. *Total neuronal cell numbers in the hippocampus ipsilateral to the site of injury were evaluated at post-HB day 30. Unbiased stereological quantifications show that mild TBI + HB caused significant neuronal cell loss in the CA1 subregion of the hippocampus and the dentate gyrus vs. the sham injury group (*p<0.05 TBI + vehicle + HB vs. sham injury; one-way ANOVA followed by Student-Newman-Keuls post hoc test). The TBI + CR8 + HB group exhibited a non-significant trend toward sham injury neuronal levels.*

6.0 DISCUSSION

The results of this study strongly support the hypothesis that exposure to AE-relevant HB within 1 week after mild to moderate TBI worsens both short- and long-term neurohistologic and neurobehavioral outcomes. Exposure of rats to 100% O_2 during the 6-hour period of HB also worsens outcomes, in comparison to those measured following HB under 21-28% O_2. These clinically highly relevant findings were observed using two very different animal models. The widely used LFP model results in moderate neurologic impairment, substantial cortical and hippocampal neuronal death, and extensive long-term neuroinflammation. The unique underbody blast model used at a level that exposes rats to 100-G acceleration results in minor neurologic impairment, little if any neuronal death, substantial axonal injury, and significant cerebrovascular injury. The fact that similar effects of HB, and exposure to 100% O_2 during HB, were observed with these different but highly combat-relevant animal models increases the concern that exposure of military or civilian TBI victims to HB during aeromedical transport may exacerbate

their injuries and could therefore be regarded as a secondary insult. Despite our confidence in the results obtained with these animal models, much more animal and clinical research must be performed before any changes in AE guidelines can be recommended.

In addition to testing for the effects of different ambient oxygen levels during HB after TBI, this study tested the hypothesis that administration of a potent anti-inflammatory agent can improve neurohistologic and neurobehavioral outcomes following TBI and exposure to HB. CR8 is a CDK inhibitor that was demonstrated previously by Dr. Faden and colleagues to reduce neuroinflammation and improve neurologic outcome in rats following TBI that were not exposed to HB [5,7]. In our study, CR8 administration after TBI and before exposure to HB inhibited microglial activation, reduced the level of brain inflammatory cytokine IL-6, reduced serum MP levels, improved neuronal survival, and improved long-term neurobehavioral outcomes. CR8 is a more potent version of roscovitine, which has shown promise as an anti-cancer agent in Phase 1 and Phase 2 clinical trials. Thus, the potential for CR8 being translated from animal TBI models to clinical trials is quite strong.

The potential impact of our current findings and those we will be generating during our new Air Force sponsored projects is underscored by the fact that approximately one-third of all Critical Care Air Transport Team transported trauma patients have been TBI victims. In light of the fact that over 3,000 military trauma victims were transported from combat zones to Landstuhl Regional Medical Center from 2001 to 2010, at least 1,000 U.S. warfighters with TBI have been exposed to potentially deleterious ambient pressures within a few days post-injury. Considering the estimate that over 300,000 U.S. service men and women had combat-related brain injuries during Operations Iraqi Freedom and Enduring Freedom, the number of U.S. military TBI victims who were exposed to HB during these conflicts is probably at least several thousand. We are therefore committed to fully understanding the effects of HB on TBI and other forms of trauma to improve the health and welfare of any future military or civilian TBI casualties who fly within days or even weeks after their injuries.

6.1 Conclusions

1. Exposure of rats to AE-relevant HB between 6 and 72 hours after blast TBI and between 6 hours and 6 days after LFP TBI worsens neuropathologic and/or neurobehavioral outcome.
2. Exposure of rats to two simulated “flights” over 3 days following LFP TBI resulted in worse neurologic outcome than that observed after a single exposure to HB.
3. Exposure to 100% O_2 during HB following either blast or LFP TBI worsens outcomes compared to the presence of 21-28% O_2.
4. The unique underbody blast model simulating vehicles targeted by improvised explosive devices results in mild TBI at accelerative G forces as low as 50 to 100 G.
    a. The histopathology of underbody blast TBI indicates axonal injury, vascular damage, and blood brain barrier disruption, which are exacerbated by exposure to HB.
    b. Blast TBI results in acute (24-hour) increase in the gene and protein expression of vWF.
    c. In contrast, the expression of the anti-apoptotic gene Bcl2 decreases substantially following blast TBI.

d. Exposure to HB following LFP TBI increases microglial activation, inflammatory cytokine levels, neuronal death, serum MP levels, and neurologic injury. Administration of CR8, a CDK inhibitor, following LFP TBI improves each of these TBI outcome markers.

6.2 Study Limitations and Way Forward

1. One species (rat), sex (male), and age (3 months) were used in this study.
   a. Future studies should compare the effects of HB after TBI using a distinctly different species, e.g., the ferret, rabbit, or pig.
   b. Studies should also compare the effects of HB after TBI using both males and females.
   c. Future studies should compare the effects of HB after TBI using immature, mature, and aged animals.
   d. One TBI severity level was used for each of the two models (i.e., mild for blast TBI and moderate for LFP TBI. Considering the data indicating that 80% of the AE TBI patients have serious to critical brain injuries, new studies should determine the effects of HB using severe animal TBI models.

2. Both animal models used in this study employed isolated TBI, with no additional injuries and no secondary insults during exposure to HB.
   a. Future studies should determine effects of AE-relevant HB on animals subjected to TBI in combination with other injuries (polytrauma).
   b. Experiments should also determine if interactions exist between HB and secondary insults, e.g., hyperthermia and hypoxia.
   c. The study did not identify a period after TBI when it is "safe to fly," i.e., when HB has no discernible effects on histologic or neurologic outcomes. Additional studies should determine if exposure to HB at 10, 14, or 20 days post-injury has deleterious effects after TBI.
   d. Only one period of 48 hours between the first and second exposures to HB was employed. Future studies should determine if a longer delay of 72 hours or 1 week is safer.
   e. The effects of oxygen during HB were only compared at two levels: 28% and 100% for LFP TBI and 21% and 100% for blast TBI. Future studies should determine if an intermediary level of oxygen, e.g., 50%, results in less injury than 100% O_2.

7.0 REFERENCES

1. Goodman MD, Makley AT, Huber NL, Clarke CN, Friend LA, et al. Hypobaric hypoxia exacerbates the neuroinflammatory response to traumatic brain injury. J Surg Res. 2011; 165(1):30-37.
2. Proctor JL, Fourney WL, Leiste UH, Fiskum G. Rat model of brain injury caused by under-vehicle blast-induced hyperacceleration. J Trauma Acute Care Surg. 2014; 77(3 Suppl 2):S83-S87.
3. Tenkova TI, Goldberg MP. A modified silver technique (de Olmos stain) for assessment of neuronal and axonal degeneration. Methods Mol Biol. 2007; 399:31-39.

4. Byrnes KR, Loane DJ, Stoica BA, Zhang J, Faden AI. Delayed mGluR5 activation limits neuroinflammation and neurodegeneration after traumatic brain injury. J Neuroinflammation. 2012; 9:43.
5. Kabadi SV, Stoica BA, Hanscom M, Loane DJ, Kharebava G, et al. CR8, a selective and potent CDK inhibitor, provides neuroprotection in experimental traumatic brain injury. Neurotherapeutics. 2012; 9(2):405-421.
6. Skovira JW, Kabadi SV, Wu J, Zhao Z, DuBose J, et al. Simulated aeromedical evacuation exacerbates experimental brain injury. J Neurotrauma. 2016 Jan 7 [Epub ahead of print].
7. Kabadi SV, Stoica BA, Loane DJ, Luo T, Faden AI. CR8, a novel inhibitor of CDK, limits microglial activation, astrocytosis, neuronal loss, and neurologic dysfunction after experimental traumatic brain injury. J Cereb Blood Flow Metab. 2014; 34(3):502-513.
8. Proctor JL, Scutella D, Pan Y, Vaughan J, Rosenthal RE, et al. Hyperoxic resuscitation improves survival but worsens neurologic outcome in a rat polytrauma model of traumatic brain injury plus hemorrhagic shock. J Trauma Acute Care Surg. 2015; 79(4 Suppl 2):S101-S109.

LIST OF ABBREVIATIONS AND ACRONYMS

AE	aeromedical evacuation
ANOVA	analysis of variance
C-STARS	Center for the Sustainment of Trauma and Readiness Skills
CA	Cornu Ammonis
CDK	cyclin-dependent kinase
CR8	2-(R)-(1-Ethyl-2-hydroxyethylamino)-6-(4-(2-pyridyl)benzyl)-9-isopropylpurine trihydrochloride
DNPH	dinitrophenylhydrazine
ELISA	enzyme-linked immunosorbent assay
FP	fluid percussion
GAPDH	glyceraldehyde-3-phosphate dehydrogenase
HB	hypobaria
HRP	horseradish peroxidase
Iba-1	ionized calcium-binding adapter molecule 1
IFN-γ	interferon gamma
IgG	immunoglobulin G
IP	intraperitoneal
LFP	lateral fluid percussion
MP	microparticle
MWM	Morris water maze
O_2	oxygen
PARP	poly-ADP-ribose polymerase
PCNA	proliferating cell nuclear antigen
RIPA	radioimmunoprecipitation assay
SDS	sodium dodecyl sulfate
TBI	traumatic brain injury
TBS	Tris-buffered saline
vWF	von Willebrand factor